Accepted Manuscript

Detecting and quantifying hydromorphology changes in a chilean river after 50 years of dam operation

Hernán Alcayaga, Sebastián Palma, Diego Caamaño, Luca Mao, Marco Soto-Alvarez

PII: S0895-9811(18)30539-X

DOI: https://doi.org/10.1016/j.jsames.2019.04.018

Reference: SAMES 2174

To appear in: *Journal of South American Earth Sciences*

Received Date: 28 December 2018

Revised Date: 22 April 2019

Accepted Date: 23 April 2019

Please cite this article as: Alcayaga, Herná., Palma, Sebastiá., Caamaño, D., Mao, L., Soto-Alvarez, M., Detecting and quantifying hydromorphology changes in a chilean river after 50 years of dam operation, *Journal of South American Earth Sciences* (2019), doi: https://doi.org/10.1016/j.jsames.2019.04.018.

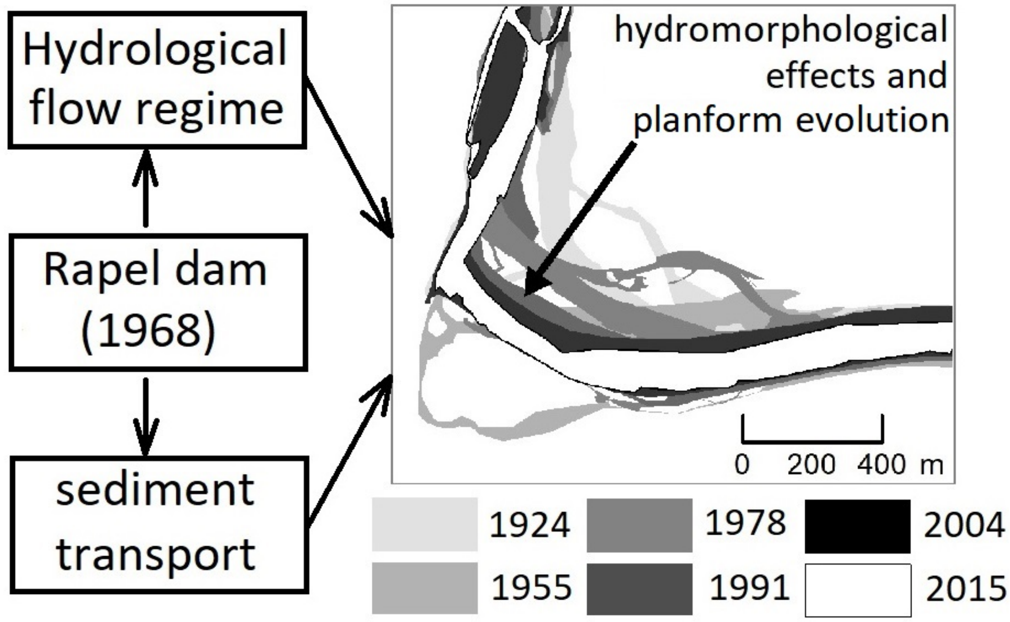

Changes in fluvial morphology due to Rapel dam

Detecting and quantifying hydromorphology changes in a Chilean river after 50 years of dam operation

Hernán Alcayaga[1]; Sebastián Palma[2]; Diego Caamaño[3]; Luca Mao[4] and Marco Soto-Alvarez[2].

(1) Assistant Professor, Dept. of Civil Engineering, Universidad Diego Portales, Chile. E-mail: hernan.alcayaga@udp.cl (hernan.alcayaga@udp.cl)

(2) Graduate Research Assistant, Dept. of Civil Engineering, Universidad Diego Portales, Chile.

(3) Associate Professor, Dept. of Civil Engineering, Universidad Católica de la Santísima Concepción, Chile; dcaamano@ucsc.cl

(4) Senior Lecturer, School of Geography, University of Lincoln, Lincoln, LN6 7TS, UK; lumao@lincoln.ac.uk

Abstract

This study identifies and characterizes hydromorphological changes along the Rapel River downstream of the first large dam built in Chile (1968). A hydromorphological analysis is carried out to assess changes on the hydrological flow regime, bed sediments, and fluvial morphology along a 19 km river reach. Results classify current global hydrological quality as "Moderate" (according to the Indicator for Hydrological Alteration in RIverS, IAHRIS), however specific indicators within this classification scheme identified quality as "Poor". The morphological quality decreased from "Very Good" to "Good" (assessed by the Morphological Quality Index, MQI). Changes in the planform were particularly intense during the post dam period when intensive lateral mobility occurred, with the corresponding loss of secondary river branches, and with generation of straighter and regular river sections with presence of an armor layer observed along the entire river reach. Between 1991 and 2015 channel stabilization with less lateral mobility was observed, which thought to be associated with the river new equilibrium trend. River width, sinuosity and braiding

index changed at different rates along the studied river reach. Our investigation demonstrates that the Rapel River experienced changes differently than those described in the literature given its lower gradient and hydraulic interaction with the Pacific Ocean.

Keyworks: Dams, human alteration, hydromorphological diagnostic**,** Rapel River

1. Introduction

Dams have been constructed since ancient times (Novak *et al.,* 2006) to develop agriculture and control water supply, and later to satisfy the needs of hydropower generation and flood protection. More than half of the world's large rivers are regulated by dams, and currently emerging countries are constructing new structures for the same agricultural and energy purposes (Nilsson *et al*., 2005). Current attempts of reducing carbon dioxide emissions in producing energy also increase the likelihood of constructing new dams. Despite this trend, several attempts in the more developed countries have emerged at exploring small and mini hydroelectric power plants. Also, the long-term impacts of old and inoperative structures led to the practice of dam removal. For example, more than 400 dams have been removed in the US (Petts and Gurnell, 2013), and a group of European countries (Sweden, Spain, Portugal, the UK, Switzerland, and France) have removed more than 3,450 weirs and dams (Dam Removal Europe, 2017). However, energy limits economic development and thus triggers a strong justification for maintaining the construction of major dams within the developing world; and these pressures are likely to grow (Oud, 2002). Hydropower dams may play an important role in climate change adaptation of water resource availability (Berga, 2016), but the environmental and social costs must be mitigated, and river hydromorphology requires inclusion in the analysis.

Large rivers in Chile drain runoff from the Andes mountain range to the Pacific Ocean responding to different geography, geology and climatic patterns along (*i.e.* North-South) and across (East-West) the country. Chilean fluvial systems spatially distribute water from the driest desert in the world in the Northern regions (Atacama Desert) to the extremely rainy areas of Patagonia in the

South. The transversal geography is abrupt and varied, as rivers flow from the Andes range to the central valley generating very high topographic gradients. For example, rivers in the Rapel basin flow from elevations close to 4500 m to 500 m within approximate 50 km resulting in average longitudinal gradient of 8%, and rapidly converting high-energy mountain rivers to low energy systems in the central valley.

Several Chilean rivers present a relatively short history of human intervention, but there are current pressures that may result is severe alteration of their morphology and dynamics (Andreoli *et al*., 2013). Despite several studies describing the effects of dams on fish habitat (Habit *et al*., 2006; Garcia *et al*., 2011; Laborde *et al*., 2016) and on the economic value of landscape loss (Ponce *et al*., 2011), very few studies have confronted the hydromorphological effects of human intervention in Chilean rivers (Arróspide *et al*., 2018; Tranmer *et al*., 2018).

During the past fifty years, fluvial geomorphologists have developed qualitative and quantitative models to predict river behavior (Wohl, 2014). One of the most relevant reasons that motivated these models is to understand channel responses to natural and human-induced disturbances. Relevantly, dams have been identified as the single most profound human alteration to fluvial systems (Grant *et al*., 2003). The changes produced by the operation of these structures can be dramatic on fluvial processes, as they are dominated by the reduction of both sediment load and flood magnitude (Buffington, 2012; Petts and Gurnell, 2013; Vietz and Finlayson, 2017). The effects of dams on fluvial hydromorphology have been measured and surveyed for more than 80 years (Lane, 1934; Williams and Wolman, 1984; Piqué *et al*., 2017) and currently, scientists and engineers have at their disposal conceptual, empirical, analytical, and numerical models to predict these changes (Grant, 2012; Alcayaga *et al*., 2018). Thus, there is a major challenge regarding the understanding of the "natural" morphological river states before the construction and operation of large dams, nonetheless, there is also a need to consider whether these alterations are reversible.

Our study seeks to identify and characterize the hydromorphological changes produced along the Rapel River downstream the only dam located in the coastal mountain range, and the first large

Chilean dam that has been operating for 50 years. Thus, based on several time-distributed data, this study described the complex response of the river due to the alterations induced by the dam on both discharge regime and sediment transfer from the upstream part of the catchment within the study area. As suggested by previous methodological works, several well-established methods were combined for addressing an analysis of the river response to impoundment. The large amount of collected data and considered parameters represents the strength of this work. The long-term hydromorphological effects of the Rapel Dam are then discussed, as each river responds to dam closure in a peculiar way due to a multitude of factors (*e.g.* morphological and sedimentological characteristics of the river, hydrological regime and dam features) and interactions between them. For this reason, this interesting case-study represents a good contribution in the challenge of increasing the dataset of analyzed situations which, in turn, represents the best way for deriving ever better general evolutionary-models of impounded rivers.

2. Material and methods

2.1. Study area

The Rapel river basin is located in central Chile (Fig. 1a) drained by an area of 13,766 km^2 that supports two main economic activities: agriculture and mining (CADE-IDEPE, 2004). The River Rapel receives its name at the confluence of two main tributaries, Tinguiririca and Cachapoal Rivers (Fig. 1b), which bring water from the Andes mountain range contributing with up to 87% of the Rapel River discharge (Benites, 1984). Hydrology and morphology impacts in this basin have being recently identified, and the main pressures are associated to irrigation and river mining taking place in the upper and middle part of the basin (CADE-IDEPE, 2004). Fig.1b shows the Rapel reservoir as a product of the Rapel dam built in the coastal mountain range in the late 60`s, storing water since 1968 and fully operational by 1971 (Balbontin, 2013). It is important to note that the Rapel Dam is the only large dam located in the mountain coastal range, as all the others are distributed along the Andes.

The Rapel hydropower plant was initially operated by the state (through the government agency ENDESA), and after privatization is currently operated by ENEL. The effective annual average water discharge is 178 m^3/s (CADE-IDEPE, 2004); during high-energy demand scenarios the turbines can supply up to 535 m^3/s (ENEL, 2017). The flow outlet is located at the dam's lower portion of the wall, with water discharge following hydropeaking operations (ENDESA, 1972). This reservoir is known by its high sedimentation rates, that between 1968 and 2010 were estimated on $159{\cdot}10^6$ m^3 for 'coarse' sediment and $18{\cdot}10^6$ m^3 for 'fine-grained' sediment (Lecaros, 2011) considering the initial water storage capacity of $697{\cdot}10^6$ m^3.

2.2. Hydrology alterations

Hydrological data prior to dam operation (define here as undisturbed discharge) was available for the period 1940 - 1966. Daily average discharge was measured at the *Puente Rapel* gauging station corresponding to the study site most upstream cross-section (Rapel Bridge, Fig. 1c). The record at this station stopped right after the dam became operational, and a short term sample of current discharge (define here as disturbed discharge) was obtained by installing a pressure sensor at the same upstream cross section (levelogger Solinst, LIM; Fig. 1c), and by calibrating a stage discharge relationship using Acoustic Doppler Current Profiler discharge measurements under different flow scenarios. This allowed for the development of a daily average discharge record for the period between May 2016 and March 2018. The measured daily average water discharge was correlated with the daily average energy produced by the Rapel hydropower plant (following Ibarra *et al.*, 2015). A second order polynomial regression resulted from this correlation defined as: $Q_d=5{\cdot}10^{-7}{\cdot}P^2 + 0.0325{\cdot}P + 5.9132$ with a correlation coefficient of $r^2 = 0.96$; where Q_d is daily discharge in m^3/s and P is mean daily power produced in MWh. This relationship allowed for the reconstruction of an average daily discharge time series for the period of 2000 to 2016, hereby denoted 'disturbed discharge'. Although this approach is subject to limitations during flood events due to the portion of discharge flowing through the spillways (not accounted as produced energy), it is considered appropriate based on ENDESA (2015) indicating this scenario as rare (*i.e.* seldom) during the time period for which discharge is approximated by the polynomial regression. A comparison between the undisturbed and disturbed discharge for a hydrological year shows that the hydrological flow regime in the Rapel River is strongly affected by dam operation (Fig. 2).

2.3. Assessment of the hydrological and morphological quality

The Rapel River downstream the dam is immediately confined by the coastal mountain range for 24 km, downstream of which channel expansion allows for channel lateral migration; and this defines the upstream boundary for our investigation along the lower 19 km of the river (Fig. 1c). This area of the Rapel receives only minor tributaries, and features an average longitudinal slope of 0.1% and a bed dominated by gravel particles downstream to the estuarine area corresponding to the last 4 km before the river reaches the Pacific Ocean, and where the substrate was identified as sand-bedded.

Several indicators and procedures available to assess the hydromorphological quality of rivers are used, most of which were developed in Europe as a response to the Water Framework Directive (*i.e.* Syrah-CE of Chandesris *et al*., 2009 in France; IHG of Ollero *et al*. 2011 in Spain; and MQI of Rinaldi *et al*., 2013 in Italy).

In this study we assessed the hydrological quality of the Rapel River using 23 indexes chosen from the original formulation of the Indicators of Hydrological Alteration in RIverS (hereon IAHRIS) developed by Martinez (2006), Martinez and Fernandez (2010), and Fernandez *et al.* (2012). These indexes are calculated from the record of daily average discharge (Q_d) and involve an extended analysis at different time scales. The IAHRIS classifies the discharge frequencies from a flow duration curve in three different classes: a) $Q_d > Q_{5\%}$ as floods (eight indexes are used); $Q_d < Q_{5\%}$ and $Q_d > Q_{95\%}$ as ordinary flow values (nine indexes are used) and; $Q_d < Q_{95\%}$ as droughts (six indexes are used). Thus the IAHRIS output is a classification of the global and partial hydrological status in five classes: high, good, moderate, poor, and bad, which are referred to a basal or reference status. In this study, the reference status is considered to the hydrological condition before dam construction (*i.e.* the aforementioned undisturbed discharge).

The morphological quality was assessed using the Morphological Quality Index (MQI) developed by Rinaldi *et al*. (2013; 2016). The calculation of MQI was made using 21 of the 28 original indicators. The MQI rates the overall hydromorphological quality with values ranging from zero (highly disturbed) to one (without alteration). These are classified into five categories: Very Poor for MQI <0.2; Poor for 0.2< MQI <0.5; Moderate for 0.5< MQI <0.7; Good for 0.7< MQI <0.85; and Very Good for MQI>0.85. The morphological condition used as the reference status was also used for the IAHRIS.

An analysis was carried out to determine whether hydropeaking has influenced the estuarine area as a land-costal transitional zone. The water levels and electrical conductivity were surveyed through the Level-Temperature-Conductivity sensors LTC1 and LTC2 (Fig.1c), discharge estimated from the LIM station readings, and tide levels obtained from the San Antonio tide gauge located approximately 40 km from the Rapel River outlet.

2.4. Bed sediment size

Samples of surface and subsurface bed sediments were taken at 28 locations along the river study reach (20 for surface analysis, and 8 considered both surface and subsurface samples). The selected locations for sampling were chosen in point bars and within the active channel (Figure 1c). Surface samples were taken by separating the surface layer with fast-drying spray paint, using the area-by-number method (Vericat *et al.*, 2006). The surface and subsurface samples where compared volume-by-weight, treating the collected surface material according to Bunte and Abt (2001) as originally proposed by Kellerhals and Bray (1971). Subsequently, the size curve for each sample was constructed and the percentiles (16th, 50th, and 84th) calculated, to finally estimate the armoring index as (D_s/D_{ss}).

2.5. Topography and aerial photos

Several surveying campaigns were realized between 2016 and 2017. First a polygonal was established based on seven reference points that were spatially distributed in order to be used as base stations for surveying the floodplain, banks and river bathymetry along the study reach. Three RTK-GPS Receivers were used, always linked to one of the predefined polygonal base stations. The vertical accuracy tolerances were set to ±15mm+1ppm for Real-time Kinematic Position (Spectra precision, Epoch 50 and 80). Bathymetry was surveyed directly with the receivers on wadable areas, and a synchronized GPS-Echosounder configuration covered the deeper portions of the river (Hi-Target, HD-380). The combination of topography and bathymetry data allowed the generation of a terrain approximation from which the 1D hydraulic geometric model was created. Bankfull field observations allowed identifying the corresponding water surface elevations, and the related discharges were back calculated through the assembled 1D hydraulic model.

One geographic map (1924) and five aerial photos (1955, 1978, 1991, 2004, and 2015) from the Chilean Military Geographical Institute (IGM) and the Chilean Aerial Photogrammetric Service (SAF) were georeferenced with an associated Total Root Mean Square Error (RMSE) of 1.4; 7.3; 5.3; 6.2; 3.1, and 2.8 m, respectively. These six images were used for a) observing changes before and after planform analyses, b) estimating changes in channel width, c) defining channel confinement, d) characterizing lateral migration of the river, e) defining braided rate, and f) calculating sinuosity. The river was divided in ten river portions (Fig. 1c). The lateral mobility of the banks along the river portions was calculated from 1955 to 2015 using the Winterbottom (2000) Method, and following the approach defined by Dewan *et al*. (2017). Sinuosity corresponds to the ratio between the length of the river following the thalweg and the distance in a straight line between the upstream and downstream end of the reach (Dey, 2014). The braiding index was calculated as twice the total length of the islands and bars divided by the mid channel river length (Brice, 1960; Pradhan *et al*., 2018). Cross sections were defined every 200 m along the river profile, and the channel banks displacements were digitalized from pairs of sequential time georeferenced photos.

2.6 Channel-forming discharge and hydraulic modeling

The channel-forming discharge is a geomorphological concept (from Ignis, 1947 to Blom *et al*., 2017) often defined as the steady state discharge able to represent the geomorphological shaping effects of a complex hydrological flow regime. As such, it is clearly a simplification of complex fluvial processes (Doyle *et al*., 2007) but can still be useful to assess channel changes in regulated rivers (*e.g*. Surian, 1999). Among other methods, the channel-forming discharge can be obtained by three different approaches (Biedenharn *et al*,, 2008): i) identifying the bankfull stage (Yan *et al*., 2017) based on cross sectional geometry associated with water discharge with field empirical observations; ii) calculating water discharge corresponding to a certain recurrence interval; and iii) calculating the effective or dominant water discharge (*i.e*. Wolman and Miller's method, 1960). In this study the first approach was used and applied for both undisturbed and disturbed hydrological regimes.

Thus, and to avoid the influence of the tide, nine cross sections located in the upper 10 km of the study reach were selected. This identification was based on a combination of channel characteristic, through field observation (visual inspection) to determine floodplain surface elevations, delineation of the limit of riparian vegetation (using aerial photos), and detection of locations where the steepness of the banks change (identified though the topography of the cross sections). To associate bankfull stage with water discharge, a 1D hydraulic model in HEC-RAS was built and calibrated (Palma, 2017). The model was calibrated using the water surface elevations obtained from the Water-Level sensors at different discharges (Fig 1c). The Manning's roughness parameter magnitude was modified to match the observed and calculated data, and the calibrated model was used to obtain the bankfull stage at each scenario (*i.e.* discharge).

3. Results

3.1. Effects of the dam closure on the hydromorphology of the Rapel River

The operational rules of the Rapel Dam severely affected the flow regime of the river in terms of habitual flow, floods, and droughts (Table 1). The magnitude of annual volumes (M1), variability of annual volumes (V1), and maximum (E1) and minimum (E2) indexes for the habitual flow condition are classified as high quality. On the contrary, for monthly discharges (magnitude and variability of the volumes), indexes M2 and V3 are classified as poor quality. This suggests that, even if the dam does not disturb the annual water volumes, the monthly volumes are severely affected. Using the criterion of water turnover rate in the reservoir defined as the ratio of reservoir capacity -CAP to the mean annual runoff - MAR (see Auel *et al.*, 2016; Sumi *et al.*, 2017), Rapel rates 0.12, and is classified as a medium CAP/MAR. This means that it does not trap large water volumes (at the annual scale). The duration and seasonality of floods (indexes IHA13 and IHA14) are not disturbed by the dam operation (high quality). However, the magnitude and variability of large floods are clearly affected (indexes IHA7 and IHA11 as poor quality). Additionally, the dam's effects on floods are particularly sensible for the variability of ordinary floods (index IHA12 classified as bad quality). The variability of the ordinary floods is classified as bad due to the hydropeaking type of operation (Figure 2a), increasing the frequency of ordinary floods. In the case of droughts, dam effects are quite strong, as revealed by indexes IHA15 to IHA19. It is important to note that the only index that shows a good quality is IHA21 (drought seasonality). The flow duration curve (Figure 2b) shows the effects on Q_d>$Q_{95\%}$ (low discharges), where the differences of the discharge magnitudes for the same percentile is largest for the rest of the discharge time series. Drought conditions (base flows) have been strongly changed, with likely important ecological consequences on the aquatic and riparian habitats (Bunn and Arthington, 2002; Pilotto *et al.*, 2018). With reference to global indexes (Table 2), the global indicator (IAG) results in a moderate hydrological status, with a lower value for droughts (IAG_D was classified as poor).

For the calculation of the Morphological Quality Index (MQI), nine river portions were considered (R1-R9; Fig. 1c). The water level records from both sensors, LTC1 and LTC2 (Fig. 3), show a sinusoidal behavior as expected in an estuarine environment (MacCready and Gyer, 2010; Rojas *et al.*, 2018). Discharge and water level signals are not in synchrony, reflecting the importance of the downstream tide control in the lower portion of the river, thus this river portion was excluded from the analysis. Confinement of the river bed was defined for each river portion and with the main geomorphological units characterized and identified. Altogether 21 sub-indicators were calculated for each year with available aerial images for the period of 1924 to 2015 (Table 3).

The values of the morphological quality for the first period 1924-1955 are defined as high for the nine sub-sections (*ca.* 0.97-0.90) and the morphological quality was classified as “Very Good”. The indicator decreased substantially after the construction of the reservoir (during 1956-1968), where values of MQI are in the range 0.80-0.71. Indeed, since 1978 the morphological quality decreased in one category and classified as “Good”. This change in the hydromorphological quality is mainly explained by the disturbance in the upstream flow and the alteration of upstream factors connected with sediments discharges (A1 and A2 according the Rinaldi *et al.*, 2016). Overall, although there was a reduction in the morphological quality due to the dam operation, the river remained in an acceptable state according to the objectives of the EU Water Framework Directive (Voulvoulis *et al.*, 2017). This alteration was maintained in subsequent years showing a stable reduction until 2015, when the MQI was “Moderate” level at R1.

3.2. Bed sediments

The sediment distribution along the lower Rapel River does not show a general tendency. Sediment size its not observed to decrease downstream (Fig. 4) as expected in natural rivers (Sternberg, 1874, Parker, 1991). Estimated trends would suggest that finer sediment (*i.e.* d_{16s}) slightly decreases in size downstream, whereas median sizes (*i.e.* d_{50s}) remained unchanged and coarser material (*i.e.* d_{84s}) indicates a mild increment in size. This finding corresponds with the stable armour layer riverbed that was found downstream the Dam. The Armour Ratio Index (ARI > 1.0) indicates that the bed is armoured along the entire study reach, especially at C3 and C5 (Table 4). Percentile 90 is shown in Table 5, and the associated transformation required for comparison is listed in the Appendix I.

3.3. Channel-forming discharge

Results are graphically presented in Figure 5 and the magnitudes for bankfull stage, bankfull discharge, and its recurrence interval for the post-dam condition are indicated in Table 6. The average bankfull discharge and associated return period were 482 m^3/s and 1.07 years, respectively.

3.4. Planform

The evolution of river planform from the last 90 years is presented through the analysis of four morphological characteristics: a) lateral movement dynamic, b) average width, c) sinuosity, and d) braiding.

3.4.1. Dynamics of lateral migration

The lateral changes of the Rapel River were evaluated using a set of six plan view images from 1924 to 2015, the same years used in the determination of the MQI. The active channel (*i.e.* main channel, secondary channels and bars) and river islands evolution are shown in Figure 6. The temporal sequence is built up using temporal polygons that represent the dynamic and adjustments for each morphological unit during the five studied periods.

The first polygon corresponds the 1924-1955 period that represents the changes in river shape for a pre-dam condition. For this first undisturbed period, the bed shows to be highly mobile in the lateral direction along eight of the nine river portions (*i.e.* R2 to R9). The next polygon (period 1955-1978) indicates lateral mobility throughout large portions of segments R2, R3, R7, R8, and R9 but with the loss of secondary channels suggesting an impact due to the estimated decrease of high flows and observed vegetation encroachment in R3. During the following period (1978-1991), additional straight and regular channels were formed, with an appreciable decrease of channel sinuosity (R7). For the last two periods (1991-2004 and 2004-2015) the overall trend is of a reduced lateral mobility, a disappearance of secondary channels (R2), an increase of stable channels, and channel narrowing. Consistent changes were observed since 1995 within the river portions R2, R3, R7, R8, and R9 in terms of lateral mobility, which are highlighted in Figure 6b showing the main direction that those changes registered on the aerial images. A different perspective for these channel migrations is provided by Figure 7 where the average rate of displacement for both river banks is considered.

3.4.2. Average channel width

The values of average channel width varying in space and time are shown in Figures 8a and 8b, respectively. Between 2004 and 2015 there is a significant decreased in river average width that is difficult to associated to a particular physical trend, with both increments and decreases, around a rather constant median value (115-145 m) and the interquartile ranges (*i.e.* 105-155 m). Additionally, from 1991 the variability of river width decreased, suggesting that the banks became more stable. The range of maximum and minimum values of width increased in the downstream direction, although the median and average values do not show a clear trend (Figure 8a). The only clear evidence is that there is an increase of average channel width starting from R7, which can likely be explained by the natural lesser confinement in the downstream direction.

3.4.3. Sinuosity and braiding index

River portions R1, R4, and R6 have both a very low sinuosity index and a negligible variation (Fig. 9a), and these are considered stable and with a natural- high confinement condition. R2 and R7 have a larger variation in sinuosity that is associated with the greater amplitude that the floodplain presents on these areas. Figure 10 indicates that the arithmetic mean and the maximum values of sinuosity (S) remain relatively constant in the time; it also shows that there is a large difference between the third quartile (Q3) and the maximum values of sinuosity, and a sustained increase in the median approaching progressively to the arithmetic mean.

The braiding index (B) did not vary much in the more stable and confined river portions R1, R4, and R6 (Fig. 10), however, there is a downstream trend showing a diminishing braiding index within the others sectors of the study reach. The reach-braiding index reaches its maximum average value in 1955, the dam was constructed in 1968 and the index shows a consistent decrease up to 2004 presenting a small increment for 2015.

River portion R2 changed planform-wise more between 1924-2015, transforming from a braided channel with longitudinal and transverse bars to a unique meandering channel with point-bars and a broad floodplain.

A summary of the analyzed morphological characteristics is shown in the previous sections (sinuosity, width and braiding index) and theirs changes in the time for each the river portions are presented in Table 7.

4. Discussion and conclusions

In this investigation, a quantitative analysis of the morphodynamic evolution of the lower Rapel River downstream of a reservoir in central Chile was carried out. The changes detected in the river - given that there are no other significant hydrological and sediment sources of disturbances from upstream- are assumed to be caused by dam operation. In addition, downstream the dam there are no major tributaries that provide water and sediment that cannot "compensate" these alterations.

The application of IAHRIS shows that the hydrological status of the 19 km-long Rapel River study reach is classified as "Moderate", and this is mainly due to the annual alteration of the water discharge defined as habitual. Thus, discharges that have not significantly changed from the original regime since the reservoir has a monthly flow regulation capacity. In contrast, at the monthly and daily scale the effects of dam operations become evident. The magnitude and variability of the monthly and daily flows have been strongly altered and were overall classified as "Poor". The former is explained by the virtual disappearance of floods, the elimination of extreme low flows, and a change in the frequency distribution of these extreme events throughout the year. For example, the maximum average discharge has decreased by 62% from 1660 m^3/s to 629 m^3/s; its coefficient of variation was modified from 54% to 19%. Therefore, in the current regime (*i.e.* disturbed), there are fewer possibilities for large floods to perform morphological work. Additionally, in selected scenarios, the hydropeaking operation came to disturb the tidal patterns in the Rapel estuary, precluding mixing and natural wave propagation.

In relation to the application of MQI, results show that there was a change in the morphological quality from "Very Good" to "Good". When estimating this index it was not possible to include the cross sectional changes since there is no river topographical information prior to dam construction.

After dam closure, total sediment storage in the reservoir was estimated to be 177 10^6 m^3 (Lecaros, 2011) including the entire grain size spectrum. Although there is no information on sediment transport conditions before the dam construction, the presence of a well-developed static armour layer suggests a reduction of sediment supply from upstream. In accordance with the above and in addition to the fact that there is only availability of coarse material (gravel) in the bed (without the possibility of significant lateral sedimentary contributions), considerable incision was expected however not observed in the field. For example, the riverbed around the six elliptical bridge piers did not show any signs of degradation. The bridge bed levels that are shown in the originals blueprints from 1952 remain with no significant change today that could be interpreted as incision.

Indeed, the reduction of sediment input from upstream can result in river incision and river narrowing. River incision as a result of damming and mining has been widely reported in a variety of climatic and geographical contexts (*e.g.* James, 1991; Kondolf, 1997; Brierley *et al.*, 2008), and there are several worldwide examples of vertical incision due to sediment deficit (*e.g.*, Rovira et al. 2005; Surian *et al*. 2009; Wyzga *et al.*, 2016; Collins *et al*., 2017), including in the Maipo river in Chile, where unmanaged in-channel gravel extraction caused considerable river narrowing and vertical incision (Arróspide *et al.*, 2018). A modest bed incision on most gravel-bed rivers below dams is generally due to the coarsening and armoring of surface sediments, which limits bed incision to values much smaller than for the finer-grained channels (Grant, 2012). The granulometric analysis determined that the bed is armored at different levels within the domain and that the size of bed materials does not vary along the channel. Williams and Wolman (1984) mention that in some regulated rivers the size distribution of the bed material for long distances in the downstream direction can be nearly constant (as in the Rapel case), but in other cases can vary considerably. In general, sediment supply downstream of dams that affects material bed size is controlled by tributary contributions and the valley geology (*e.g.* supply from landslides, rockfalls, and river banks). This river reach does not have important tributaries, but there are vestiges of several sources of sediments from old landslides and riverbank erosion. The sediment supply from these sources is composed by fine sediments (Fig. 11), characteristic of the coastal mountain range (Mathieu *et al.*, 2007). These fine sediments are transported by suspension to the estuarine zone and ocean, hence this sediment supply is not relevant in terms of bed sediment. Static armour layers have been observed when the delivery of bed material to a given reach is lower than the river's capacity to transport that material (*e.g.* Dietrich *et al*., 1989; Hassan and Church, 2000), which occurs in the presence of dams with no other sources of supply. Indeed, armoring as a result of limited sediment supply conditions is widely reported in the literature (Surian *et al.* 2009; Wyzga *et al.*, 2012) as a mechanism that can re-establish the dynamic equilibrium of rivers. In extreme cases, alluvial rivers also incise until the profile eventually reaches bedrock (*e.g.* Hajdukiewicz *et al*., 2017). In the Rapel River, an armour layer was formed as consequence of selective transport, due to the decrease in the magnitude of peak water discharge and upstream sediment supply. This explains the uniform distribution of the surface sediments size downstream.

In the analysis of the temporal dynamics of the planform, two periods of change have been identified. The greatest lateral mobility occurred between 1955 and 1991 (*i.e.* first period), with loss of secondary river branches and with a tendency towards the generation of straighter and regular river portions. A second period is identified between 1991 and 2015, and it represents a more stable channel condition with less lateral mobility and with adjustments only within the path established in the previous period. The width, sinuosity and braiding changed at different rates along the study reach. The planform pattern was characterized by a slight downstream increment in width but almost no change in sinuosity. Braiding decreased downstream, which is considered to be associated with a new dynamic equilibrium from downstream (*e.g.* Tranmer *et al.*, 2018).

Planform changes were particularly intense during the initial 1955-1991 period. However, the magnitude of the morphological response for the entire 1955-2015 period was not as high as expected. For example, when comparing the average, entire-reach pre dam) and post dam values, the percentage decrease in width, sinuosity, and braided index was 29%, 1%, and 50%, respectively. The section most sensitive to changes in flow and sediment was R2, where the bed is currently narrower and less mobile, with a single and fixed channel.

The temporal dynamics are characterized by changes that were manifested almost immediately after dam construction and operation, with several case studies supporting this evidence (Williams and Wolman, 1984; Petts, 1984; Church, 1995; Petts and Gurnell, 2013). The changes that occur during the first decades after dam construction correspond to a characteristic response of alluvial rivers, with high sediment loads and with a rapidly growth of woody vegetation (Petts and Gurnell, 2013). In the Rapel River, changes in the geometry and distribution of sediment grain size in the bed seem to have stabilized. Measurements of the bedload transport with a Helley Smith during floods (hydropeaking) for discharges from 220 to 510 m^3/s (the average bankfull discharge was 482 m^3/s, see Table 6), showed that the transport is minimal and only mobilized a small fraction of the diameters (1.68 - 4.76 mm). This could be associated with a current fixed bed given the static armour layer, suggesting that the Rapel River downstream the dam has already reached its new post-dam quasi-equilibrium state (Petts and Gurnell, 2005). Consequently, if the current hydrological and sedimentary conditions do not undergo significant modifications (they remain under the geomorphic thresholds, according to Church 2002, Schumm, 1979; Schumm 1977), the morphological characteristics of the Rapel river should not have significant changes. In this sense, a short reaction time was observed and based in Petts and Gurnell (2005), the trajectory of the river evolution is at the end of the relaxation time. In terms of Gregory's (2006) theoretical framework, the Rapel fluvial system is not significantly sensitive to the alterations caused by the dam on hydrology regime and sediment dynamic.

One limitation in this study was is that no cross sectional data for the pre-dam period were available, making the interpretation of the results more difficult. No stream gauges were available at the study reach for the post-dam period, and the discharges time series were obtained by an indirect method, which may have underestimated high flows.

The hydromorphological effects of dams are site-specific and depend also on the type of operation of the reservoir. The morphological response of rivers to dams vary depending on location, environment, substrate, water release, and sediment load (Brandt, 2000). According to Grant (2012; p.177): "Every river is different, every dam is unique, and understanding the impact of the latter on the former will always have an element of art to complemented the science". Thus, each evaluation delivers somewhat different results. We verify that the construction and operation of the Rapel Dam disrupted the continuity of flow and sediment transport downstream, affecting the morphology of the channels and its dynamics. The hydromorphological consequences of altering these flows have been smaller than expected, possibly in part because of the small longitudinal slope of the river. Although these impacts were not particularly severe, they were sufficient to ensure that the river does not longer holds a "Very Good" hydromorphological quality status, meaning that its behavior does not correspond to a natural fluvial system.

Acknowledgements: This study was supported by FONDECYT project n. 11140764: "Time and space scales in the morphological responses of river morphology due to large structures (hydropower): approaches to better understanding the trends and kinetic responses of the rivers in Chile", funded by the Chilean National Agency for the Science and Technology (CONICYT), and grant UCSC-FAA N416/2018, Chile.

References

Alcayaga, H., Mao, L., Belleudy, Ph., 2018. Predicting the geomorphological responses of gravel bed rivers to flow and sediment source perturbations at the watershed scale: an application in an Alpine watershed. Earth Surf. Process. Landforms 43, 894–908. https://doi.org/10.1002/esp.4278

Andreoli, A., Mao, L., Iroumé, A., Arumí, J., Nardini, A., Pizarro, P., Caamaño, D., Meier, C., Link, O., 2013. The need for a hydromorphological approach to Chilean river management. Revista Chilena de Historia Natural 85: 339-343.

Arróspide, F., Mao, L., Escauriaza, C., 2018. Morphological evolution of the Maipo in central Chile: Influence of instream gravel mining. Geomorphology, 306, 182-197.

Auel, C., Kantoush, SA., Sumi, T., 2016. Positive effects of reservoir sedimentation management on reservoir life, example from Japan. In: International Symposium on “Appropriate Technology to ensure Proper Development, Operation and Maintenance of Dams in Developing Countries”, Johannesburg, South Africa, SANCOLD, ISBN 978-0-620-71042-8

Balbontin, J.E., 2013. Modelación de la sedimentación del embalse Rapel: Delta y corriente de turbidez. Memoria de Ingeniero Civil, Universidad De Chile. (In Spanish)

Benites, A., 1984. Estimación de la sedimentación en el embalse Rapel, ENDESA. División Estudios Hidrológicos. (In Spanish)

Berga L., 2016. The role of hydropower in climate change mitigation and adaptation: A review. Engineering, Vol 2, Issue 3, 313-318, ISSN 2095-8099. doi: 10.1016/J.ENG.2016.03.004.

Biedenharn, D.S, Watson, C.C, Thorne, C.R., 2008. Fundamentals of fluvial geomorphology. In Sedimentation Engineering. Processes, Measurements, Modeling and Practice, Chapter 6, Garcia M (ed). American Society of Civil Engineers; 355–386 https://doi.org/10.1061/9780784408148.ch06#sthash.8mMb237m.dpuf.

Blom, A., Arkesteijn L., Chavarrías V, Viparelli E., 2017. The equilibrium alluvial river under variable flow and its channel-forming discharge, Journal of Geophysical Research. Earth Surface., 122, 1924–1948, doi:10.1002/2017JF004213.

Brandt, S.A., 2000. Prediction of downstream geomorphological changes after dam construction: a stream power approach. International Journal of Water Resources Development, 16(3), 343-367.

Brice, J. C., 1960. Index for description of channel braiding. Geological Society of America Bulletin, 71, 1833.

Brierley, G., K. Fryirs, A. Boulton, and C. Cullum., 2008. Working with change: the importance of evolutionary perspectives in framing the trajectory of river adjustment. Pages 65-84 in G. Brierley and K. Fryirs, editors. River Futures: An Integrative Scientific Approach to River Repair. Island Press, Washington, D.C., USA.

Buffington, J.M., 2012. Changes in channel morphology over human time scale. In Gravel-Bed Rivers: Processes, Tools, Environments, Church M, Biron P, Roy A (eds), 1st edn. John Wiley & Sons.

Bunn, S.E. and Arthington, A.H., 2002. Basic principles and ecological consequences of altered flow regimes for aquatic biodiversity. Environmental Management, 30, 492-507. doi:10.1007/s00267-002-2737-0

Bunte, K and Abt, S. 2001. Sampling surface and subsurface particle-size distributions in wadable gravel-and cobble-bed streams for analyses in sediment transport, hydraulics, and streambed monitoring. Gen. Tech. Rep. RMRS-GTR-74. Fort Collins,CO: U.S. Department of Agriculture, Forest Service, Rocky Mountain Research Station. 428 p.

Cade-Idepe, 2004. Diagnóstico y clasificación de los cursos y cuerpos de agua según objetivos de calidad, Cuenca del río Rapel (In spanish). Available in: http://portal.mma.gob.cl/wp-content/uploads/2017/12/Rapel.pdf

Chandesris, A., Malavoi, J.R., Mengin, N., Wasson, J.G., Souchon, Y., 2009. Hydromorphology auditing: a generalized framework at a nation scale to view streams and rivers in their landscape context. The 7th International Symposium on Ecohydraulics, Concepcion, Chile. (1-9 pp).

Church, M., 1995. Geomorphic response to river flow regulation: Case studies and time scales. Regul. Rivers: Res. Mgmt., 11: 3-22. doi:10.1002/rrr.3450110103

Church, M. 2002. Geomorphic threshold in riverine landscapes. Freshwater biology 47, 541-557.

Collins, M. J., Snyder, N. P., Boardman, G., Banks, W. S. L., Andrews, M., Baker, M. E., Conlon, M., Gellis, A., McClain, S., Miller, A., and Wilcock, P. (2017) Channel response to sediment release: insights from a paired analysis of dam removal. Earth Surf. Process. Landforms, 42: 1636–1651. doi: 10.1002/esp.4108.

Dam removal Europe, 2017. Website http://damremoval.eu/ [Accessed 11 Nov. 2018]

Dewan, A., Corner, R., Saleem, A., Rahman, M.M., Haider, M.R., Rahman, M.M., Sarker, M.H., 2017. Assessing channel changes of the Ganges-Padma River system in Bangladesh using Landsat and hydrological data. Geomorphology, 276, 257-279.

Dey, S. 2014. Fluvial Hydrodynamics, Hydrodynamic and Sediment Transport Phenomena; Springer Publisher. ISBN 978□3□642□19061□2

Dietrich, W., Kirchner, J., Ikeda, H., and Iseya, F., 1989. Sediment supply and the development of the coarse surface layer in gravel-bedded rivers, Nature, 340, 215–217.

Doyle, M., Shields, F., Boyd, K., Skidmore, P., Domminick, D., 2007. Channel-forming discharge selection in river restoration design. Journal of Hydraulic Engineering 133: 831–837.

Emmett, W. W. 1979. A field calibration of the sediment-trapping characteristics of the Helley-Smith bedload sampler (Vol. 1139). US Government Printing Office.

ENDESA, 1972. Rapel. folleto descriptivo del funcionamiento de la Central Rapel. (In Spanish) Available in: http://www.memoriachilena.cl/archivos2/pdfs/MC0037323.pdf

ENDESA. 2015. Datos estadísticos evacuaciones por exceso y tiempo de evacuación desde el año 1975 al 2006. (In Spanish)

Enel, 2017. Central Rapel (Chile). [Accessed 13 Aug. 2018] http://www.enelgeneracion.cl/es/conocenos/nuestroNegocio/centrales/Paginas/centralrapel.aspx

Fernández, J., Martínez, C., Magdaleno, F., 2012. Application of indicators of hydrologic alterations in the designation of heavily modified water bodies in Spain, Environmental Science & Policy, Vol16, 2012, pp 31-43. doi.org/10.1016/j.envsci.2011.10.004.

García, A., Jorde, K., Habit, E., Caamaño, D., Parra, O., 2011. Downstream environmental effects of Ralco and Pangue dam operations: Changes in habitat quality for native fish species, Biobío River, Chile. River Research and Applications. Vol. 27, Issue 3, pp 312 – 327.

Grant, G.E., Schmidt, J.C., Lewis, S.L., 2003. A geological framework for interpreting downstream effects of dams on rivers: In a peculiar river, water science and application 7. O'Connor JE, Grant GE. (eds.) Washington, D.C., American Geophysical Union, pp. 203-219.

Grant, G., 2012. The geomorphologic responses gravel-bed rivers to dams: perspectives and prospects. In: Church, M.; Biron, PM: Roy, AG. Eds. Gravel-Bed Rivers: processes, tools, environments. Chichester, UK: John Wiley & Sons, Ltd, pp.165-181.

Gregory, K.J., 2006. The human role in changing river channels, Geomorphology, Volume 79, Issues 3–4, (172-191). https://doi.org/10.1016/j.geomorph.2006.06.018.

Habit, E., Belk, M., Tuckfield, C., Parra, O., 2006. Response of the fish community to human-induced changes in of the Biobio river in Chile. Freshwater Biol. 51, 1–11.

Hajdukiewicz, H., Wyżga, B., Zawiejska, J. et al., 2017. Assessment of river hydromorphological quality for restoration purposes: an example of the application of RHQ method to a Polish Carpathian river. Acta Geophys. 65: 423. https://doi.org/10.1007/s11600-017-0044-7

Hassan, M.A., Church, M., 2000. Experiments on surface structure and partial sediment transport on a gravel bed. Water Resources Research, 36(7), pp 1885- 1895

Ibarra, G., de la Fuente A., Contreras, M., 2015. Effects of hydropeaking on the hydrodynamics of a stratified reservoir: the Rapel Reservoir case study, Journal of Hydraulic Research. DOI: 10.1080/00221686.2015.1060271

Ignis, C., 1947. Meanders and their bearing on river training. Paper N.7, Institution of Civil Engineers, Maritime and waterways engineering Division, London.

James A., 1991. Incision and morphologic evolution of an alluvial channel recovering from hydraulic mining sediment. GSA Bulletin;103 (6): 723–736. doi: https://doi.org/10.1130/0016-7606(1991)103<0723:IAMEOA>2.3.CO;2

Kellerhals, R., and Bray, D. I. 1971. Sampling procedures for coarse fluvial sediments. Journal of the Hydraulics Division. American Society of Civil Engineers97, 1165-1180.

Kondolf, G.M., 1997. Hungry Water: Effects of dams and gravel mining on river channels, Environmental Management, 21(4): 533-551.

Laborde, A., González, A., Sanhueza, C., Arriagada, P., Wilkes, M., Habit, E., Link, O., 2016. Hydropower development, riverine connectivity and non-sport fish species: Criteria for hydraulic design of fishways”. River Research and Applications 32(9):1949-1957.

Lane, E.W., 1934. Retrogression of levels in riverbeds below dams: Engineering News-Records, v.112, p. 836-388.

Lecaros, M., 2011. Estudio de sedimentación en el embalse Rapel. Memoria para optar al título de ingeniero civil, Universidad de Chile. (In Spanish) www.cybertesis.uchile.cl/tesis/uchile/2011/cf-lecaros_ms/pdfAmont/cf-lecaros_ms.pdf

MacCready, P., Geyer, W.R., 2010. Advances in Estuarine Physics. Annual Review of Marine Science, 2(1), 35–58. doi:10.1146/annurev-marine-120308-081015

Martínez, C., Fernández, J.A., 2010. IAHRIS 2.2 Índices de alteración hidrológica en ríos. Manual de referencia metodológica. Available in: http://www.ecogesfor.org/pdf/MANUAL_USUARIO_IAHRIS_v2-2.pdf

Martínez, C., 2006. El régimen natural de caudales: una diversidad imprescindible, una diversidad predecible. Revista Invest Agrar: Sist Recur For Fuera de Serie, 15(1), 153-165.

Mathieu, R., Cervelle, B., Rémy, D., Pouget, M., 2007. Field-based and spectral indicators for soil erosion mapping in semi-arid mediterranean environments (Coastal Cordillera of central Chile). Earth Surf. Process. Landforms, 32: 13–31. doi:10.1002/esp.1343

Nilsson, C., Reidy CA., Dynesius M., Revenga C., 2005. Fragmentation and flow regulation of the world's large river systems. Science, 308(5720), 405–408. doi:10.1126/science.1107887

Novak, P., Moffat, A.I.B., Nalluri, C., Narayanan, R., 2006. Hydraulic Structures. Fourth edition published by Taylor & Francis. London. ISBN 10: 0415386268

Oud, E., 2002. The evolving context for hydropower development. Energy Policy 30: 1215–1223.

Ollero, A., Ibisate, A., Gonzalo, L.E., Acín, V., Ballarín, D., Díaz, E., Domenech, S., Gimeno, M., Granado, D., Horacio, J., Mora, D., Sánchez Fabre, M., 2011. The IHG index for hydromorphological quality assessment of rivers and streams: updated version. Limnetica, 30 (2): 225-262. DOI: 10.23818/limn.30.19

Palma, S. 2017. Identificación de cambios hidromorfológicos del río rapel aguas abajo de la central Rapel, Master thesis. Universidad Diego Portales.(In Spanish)

Parker, G., 1991. Selective sorting and abrasion of river gravel. II: Applications. Journal of Hydraulic Engineering, 117(2), 150-171.

Petts, G.E., 1984. Impounded rivers. Perspectives for Ecological Management. John Wiley & Sons, Chichester, UK, 326 pp.

Petts, G.E., and Gurnell, A.M. 2005. Dams and geomorphology: Research progress and future directions. Geomorphology, 71(1-2), 27–47. doi:10.1016/j.geomorph.2004.02.015

Petts, G., Gurnell, A., 2013. Hydrogeomorphic effects of reservoirs, dams, and diversions. In Treatise on Geomorphology, Shroder J, (Editor in Chief), Wohl E (ed). Academic Press, San Diego CA. Vol 13, Fluvial Geomorphology, 96–113.

Pilotto, F. , Tonkin, J. D., Januschke, K. , Lorenz, A. W., Jourdan, J. , Sundermann, A. , Hering, D. , Stoll, S. and Haase, P., 2018. Diverging response patterns of terrestrial and aquatic species to hydromorphological restoration. Conservation Biology. doi:10.1111/cobi.13176

Piqué, G., Batalla, R.J., López, R., Sabatera, S. 2017. The fluvial sediment budget of a dammed river (upper Muga, southern Pyrenees). Geomorphology 293, 211-226. https://doi.org/10.1016/j.geomorph.2017.05.018

Ponce, R., Vásquez, F., Stehr, A., Debels, P., Orihuela, C., 2011. “Estimating the economic value of landscape losses due to flooding by hydropower plants in the Chilean Patagonia” Water Resource Management, 25, 2449-2466.

Pradhan, C., Chembolu, V., Dutta, S., 2018. Impact of river interventions on alluvial channel morphology, ISH Journal of Hydraulic Engineering, DOI: 10.1080/09715010.2018.1453878

Rinaldi, M., Surian, N., Comiti, F., Bussettini, M., 2013. A method for the assessment and analysis of the hydromorphological condition of Italian streams: the Morphological Quality Index (MQI). Geomorphology, 180-181, 96-108.

Rinaldi, M., Surian, N., Comiti, N., Bussettini, M., Gurnell, A.M., 2016. Guidebook for the evaluation of stream morphological conditions by the Morphological Quality Index (MQI). ISPRA.

Rojas, O., Mardones, M., Martines, C., Flores, L., Sáez K., Araneda, A., 2018. Flooding in Central Chile: Implications of Tides and Sea Level Increase in the 21st Century. Sustainability, 10, 4335; doi:10.3390/su10124335

Rovira, A., Batalla, R. J. and Sala, M., 2005. Response of a river sediment budget after historical gravel mining (the lower Tordera, NE Spain). River Res. Applic., 21: 829-847. doi:10.1002/rra.885

Schumm S.A. 1977. The Fluvial System. Wiley-Interscience, New York, 338pp.

Schumm, S.A. 1979. Geomorphic thresholds: the concept and its applications, Transactions of the Institute of British Geographers., NS4, 485–515.

Surian, N., 1999. Channel changes due to river regulation: the case of the Piave River, Italy. Earth Surf. Process. Landforms, 24: 1135–1151. doi: 10.1002/(SICI)1096-9837(199911)24:12<1135::AID-ESP40>3.0.CO;2-F

Surian, N., Rinaldi, M., Pellegrini, L., Audisio, C., Maraga, F., Teruggi, L., Turitto, O., and Ziliani, L., 2009. Channel adjustments in northern and central Italy over the last 200 years, in James, L.A., Rathburn, S.L., and Whittecar, G.R., eds., Management and Restoration of Fluvial Systems with Broad Historical Changes and Human Impacts: Geological Society of America Special Paper 451, p. 83–95, doi: 10.1130/2009.2451(05)

Sumi, T., Kantoush S., Esmaeilli, T., Ock, G., 2017. Sediment Flushing and replenishment below dams: Insights from Japanese case studies. In: Gravel-Bed Rivers: Processes and Disasters, First Edition. Tsursumi D. and Laronne J. (Eds.). John Wiley & Sons Ltd.

Sternberg, H., 1875. Untersuchungen über Länger-und querprofil geschiebeführender, Flüisse: Zeitschrift für Bauwesen, v. 25, pp 483-506 (In German).

Tranmer, A., Goodwin, P., Caamaño, D., 2018. Assessment of alluvial trends toward dynamic equilibrium under chronic climatic forcing. Advances in Water Resources, 120, 19-34.

Vericat, D., Garcia, C., y Batalla, R. J. 2006. Variaciones temporales y espaciales en la granulometría del tramo bajo del Ebro. Cuaternarío y geomorfología, 20(1-2), 47-60

Vietz, G.J. and Finlayson, B.L., 2017. Geomorphological Effects of Flow Alteration on Rivers. Water for the Environment, 83–100. doi:10.1016/b978-0-12-803907-6.00005-x

Voulvoulis, N., Dominic, K., Giakoumis, T., 2017. The EU Water Framework Directive: From great expectations to problems with implementation. Science of The Total Environment, 575, 358-366. doi.org/10.1016/j.scitotenv.2016.09.228.

Williams, G.P., Wolman, M.G., 1984. Downstream Effects of Dams on Alluvial Rivers. US Geological Survey, 83p.

Winterbottom, S., 2000. Medium and short-term channel planform changes on the Rivers Tay and Tummel, Scotland. Geomorphology, 34(3-4), 195-208.

Wohl, E., 2014. Time and the rivers flowing: fluvial geomorphology since 1960. Geomorphology. 216: 263–282. https://doi.org/ 10.1016/j.geomorph.2014.04.012.

Wolman, M.G., Miller, J.P., 1960. Magnitude and frequency of forces in geomorphic processes. The Journal of Geology, 68(1), 54-74.

Wyżga B, Zawiejska J, Radecki-Pawlik A, Hajdukiewicz H., 2012. Environmental change, hydromorphological reference conditions and the restoration of Polish Carpathian rivers. Earth Surf Process Landforms 37:1213–1226. doi: 10.1002/esp.3273

Wyżga B., Zawiejskab J., Radecki-Pawlikc A, 2016. Impact of channel incision on the hydraulics of flood flows: Examples from Polish Carpathian rivers. Geomorphology, 272, pp10-20. https://doi.org/10.1016/j.geomorph.2015.05.017

Yan, Q., Iwasaki, T., Stumpf, A., Belmont, P., Parker, G., Kumar, P., 2017. Hydrogeomorphological differentiation between floodplains and terraces. Earth Surf. Process. Landforms, doi: 10.1002/esp.4234.

FIGURE CAPTIONS

Figure 1. (a) Location of the Rapel Basin along the Chilean geographic context; (b) the Rapel River Basin and Rapel Dam location also indicate the complete reach under study; and (c) river study reach.

Figures 2. Comparison between (a) the daily average water discharges for undisturbed (1966) and disturbed conditions (2016), and (b) comparison between the daily flow duration curves for undisturbed (1940-1966) and disturbed time series (2000-2016).

Figure 3. Records of discharge at LIM station and water levels at TLC1 and TLC2 stations

Figure 4. Grain size distribution downstream trends for d_{16}, d_{50} and d_{84}.

Figure 5. Bankfull stages (XS) and 1D hydraulic model cross sections. XSs for the bankfull stages are presented in the upper right graphs, where L and R indicate the left and the right banks, respectively. The results for the 1D hydraulic model are presented in terms of water depth for the average bankfull discharge (482 m^3/s).

Figure 6. (a) Planform evolution of the Rapel River between 1924 and 2015, and (b) a five detail graphics for those places where the lateral movement was significant.

Figure 7. Average rates of lateral displacement for the left and the right riverbanks.

Figure 8. Average river widths variations in space (a) and time (b). In the box-and-whiskers plots the extreme values are the minimum and maximum widths (whiskers), the extremes values of the

box are lower quartile (Q1) and upper quartile (Q3), the box division line represent the median value (Q2), whereas the point marker corresponds to the mean value.

Figure 9. Spatial (a) and temporal (b) variations of average sinuosity index.

Figure 10. Spatial (a) and temporal (b) variations of average braiding index.

Figure 11. Typical geologic context in the mountain coastal range, with limited coarse sediments sources (this photo correspond to the river portion R3 for Fig.1c).

TABLES

Table 1. Results for IAHRIS method, partial index

Table 2. Results for IAHRIS method, global index

Table 3. Results for MQI method per year, river portion, and a global quality index

Table 4. Armour Ratio Index (ARI)

Table 5. d_{90} for surface and sub-surface samplers

Table 6. Bankfull stage, discharges associated and recurrence interval

Table 7. Spatial and temporal morphological configuration in terms of observed sinuosity (S), average width (W) and braiding index (B) separated by river portion.

APPENDIX I.

Table I. Required transformation to compared surface with subsurface samples.

Sample	Surface	Sub-surface
1	Conversion of area-by-weight to volume-by- weight (conversion factor 1/D)	Volume-by-weight
2	Conversion of area-by-weight to volume-by-weight (conversion factor 1/D)	Volume-by-weight
3	Volume-by- weight	Volume-by-weight
4	Conversion of area-by- weight to volume-by-weight (conversion factor 1/D)	Volume-by-weight
5	Conversion of area-by- weight to volume-by-weight (conversion factor 1/D)	Volume-by-weight
6	Conversion of area-by- weight to volume-by-weight (conversion factor 1/D)	Volume-by-weight
7	Volume-by-weight	Volume-by-weight
8	Volume-by-weight	Volume-by-weight

	IAHRIS Codes	Index name	Index value	Status Classification
Habitual flow values	M1	Magnitude of annual volumes	0.85	High
	M2	Magnitude of monthly volumes	0.33	Poor
	M3	Magnitude of volume for each month	0.33	Poor
	V1	Variability of annual volumes	0.93	High
	V2	Variability of monthly volumes	0.37	Poor
	V3	Variability of volume for each month	0.37	Poor
	V4	Extreme variability index	0.28	Poor
	E1	Maximum seasonality	0.83	High
	E2	Minimum seasonality	1.00	High
Floods	IAH7	Magnitude of large floods	0.38	Poor
	IHA8	Magnitude of bankfull discharges	0.55	Moderate
	IHA9	Magnitude of connectivity discharges	0.31	Poor
	IHA10	Magnitude of flushing discharges	0.77	Good
	IHA11	Variability of large floods	0.35	Poor
	IHA12	Variability of ordinary floods	0.07	Bad
	IHA13	Flood duration	0.93	High
	IHA14	Flood seasonality	0.90	High
Droughts	IHA15	Magnitude of extreme drought	0.17	Bad
	IHA16	Magnitude of ordinary drought	0.21	Poor
	IHA17	Variability of extreme drought	0.35	Poor
	IHA18	Variability of ordinary drought	0.00	Bad
	IHA19	Drought duration	0.54	Poor
	IHA21	Drought seasonality	0.74	good

IAHRIS Codes	Index name	Global value	Status Classification
IAG_H	Global Habitual flow Index	0.34	Moderate
IAG_F	Global Floods Index	0.27	Moderate
IAG_D	Global Droughts Index	0.10	Poor
IAG	Global Alteration Index	0.25	Moderate

Year	River segments									
	R1	R2	R3	R4	R5	R6	R7	R8	R9	Global quality
1924	VG(0.92)	VG(0.95)	VG(0.93)	VG(0.92)	VG(0.93)	VG(0.92)	VG(0.97)	VG(0.92)	VG(0.93)	VG(0.93)
1955	VG(0.91)	VG(0.92)	VG(0.91)	VG(0.95)	VG(0.93)	VG(0.90)	VG(0.95)	VG(0.90)	VG(0.93)	VG(0.92)
1978	G(0.76)	G(0.76)	G(0.71)	G(0.80)	G(0.78)	G(0.80)	G(0.78)	G(0.78)	G(0.73)	G(0.77)
1991	G(0.76)	G(0.73)	G(0.81)	G(0.78)	G(0.81)	G(0.80)	G(0.79)	G(0.74)	G(0.78)	G(0.78)
2004	G(0.73)	G(0.78)	G(0.78)	G(0.75)	G(0.76)	G(0.78)	G(0.82)	G(0.74)	G(0.78)	G(0.77)
2015	M(0.68)	G(0.76)	G(0.73)	G(0.72)	G(0.73)	G(0.72)	G(0.77)	G(0.70)	G(0.76)	G(0.73)

VG: Very Good quality, G: Good quality, and M: Moderate quality.

	$d_{50\ surface}$	$d_{50\ sub\text{-}surface}$	ARI
C1	23.2	20.3	1.1
C2	20.8	12.5	1.7
C3	41.7	16.3	2.6
C4	13.8	11.7	1.2
C5	35.3	13.8	2.6
C6	22.3	14.6	1.5
C7	37.4	20.1	1.9
C8	23.7	13.0	1.8

D90	1	2	3	4	5	6	7	8
Surface	55.89	34.73	57.36	46.70	58.73	43.90	69.00	53.15
Sub-surface	47.69	24.22	24.90	53.42	29.62	30.55	47.61	30.25

XS	River Bank	Criteria for bankfull stage identification: Topography	Aerial photos	Field observation	Results: Bankfull stage (m)	Bankfull dischage (m^3s^{-1})	Recurrence interval (yr)
1	L	N	N	N	7.17	417	1.02
	R	N	Y	Y			
2	L	Y	Y	Y	6.27	322	1.00
	R	N	Y	Y			
3	L	Y	Y	N	5.50	400	1.01
	R	N	Y	N			
4	L	N	Y	Y	5.15	469	1.05
	R	N	Y	Y			
5	L	Y	Y	N	4.44	413	1.02
	R	N	Y	N			
6	L	Y	N	Y	3.24	470	1.05
	R	N	N	N			
7	L	N	N	N	2.50	579	1.31
	R	Y	Y	Y			
8	L	Y	Y	N	2.89	598	1.41
	R	Y	Y	N			
9	L	Y	Y	N	2.60	662	1.99
	R	N	N	N			

XS: control cross section for bankfull stage identification; L: left bank; R: right bank; N: It was not possible to identify the bankfull stage with this criteria; Y: it was possible to identify the bankfull station with this criteria

Portions of river	1924			1955			1978			1991			2004			2015		
	S	W	B	S	W	B	S	W	B	S	W	B	S	W	B	S	W	B
R1	1,0	141,8	0,0	1,0	139,8	0,0	1,0	144,0	0,0	1,0	159,5	0,0	1,0	157,3	0,0	1,0	85,3	0,0
R2	1,2	142,9	2,4	1,6	102,4	3,1	1,4	132,3	2,3	1,5	133,5	1,2	1,6	131,0	0,4	1,6	86,7	1,0
R3	2,3	99,8	1,1	2,2	132,9	2,3	2,1	122,0	0,7	2,2	105,3	0,3	2,2	118,0	0,0	2,2	74,9	0,2
R4	1,0	123,3	0,0	1,0	106,0	0,0	1,0	107,0	0,0	1,0	124,8	0,0	1,1	160,0	0,0	1,0	85,2	0,0
R5	1,3	128,8	0,4	1,2	92,5	0,0	1,3	121,2	0,0	1,2	118,0	0,5	1,2	136,8	1,1	1,3	65,1	1,2
R6	1,0	197,0	0,0	1,1	113,0	0,0	1,0	120,7	0,0	1,0	105,0	0,0	1,1	115,3	0,0	1,0	61,8	0,1
R7	1,1	140,5	0,0	1,5	72,3	1,6	1,5	126,0	0,0	1,2	100,7	0,0	1,2	114,5	0,1	1,3	60,7	1,2
R8	1,0	149,7	0,7	1,1	125,0	0,5	1,1	186,9	0,0	1,2	115,3	0,0	1,2	132,3	0,0	1,2	74,4	0,0
R9	1,3	131,6	0,0	1,1	139,1	0,0	1,2	223,9	0,3	1,2	156,8	0,1	1,3	156,3	0,0	1,3	132,3	0,1

S: Sinuosity; W: average width (m) and B: Braiding index

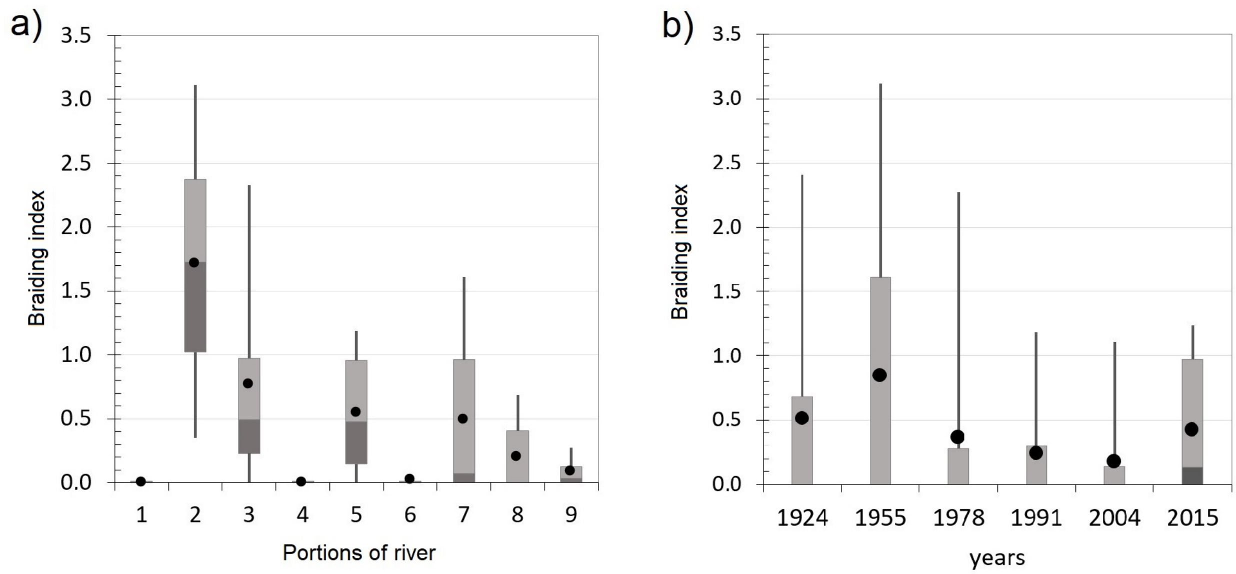
a)
3.5
3.0
2.5
2.0
1.5
1.0
0.5
0.0
Braiding index
1 2 3 4 5 6 7 8 9
Portions of river
b)
3.5
3.0
2.5
2.0
1.5
1.0
0.5
0.0
Braiding index
1924 1955 1978 1991 2004 2015
years

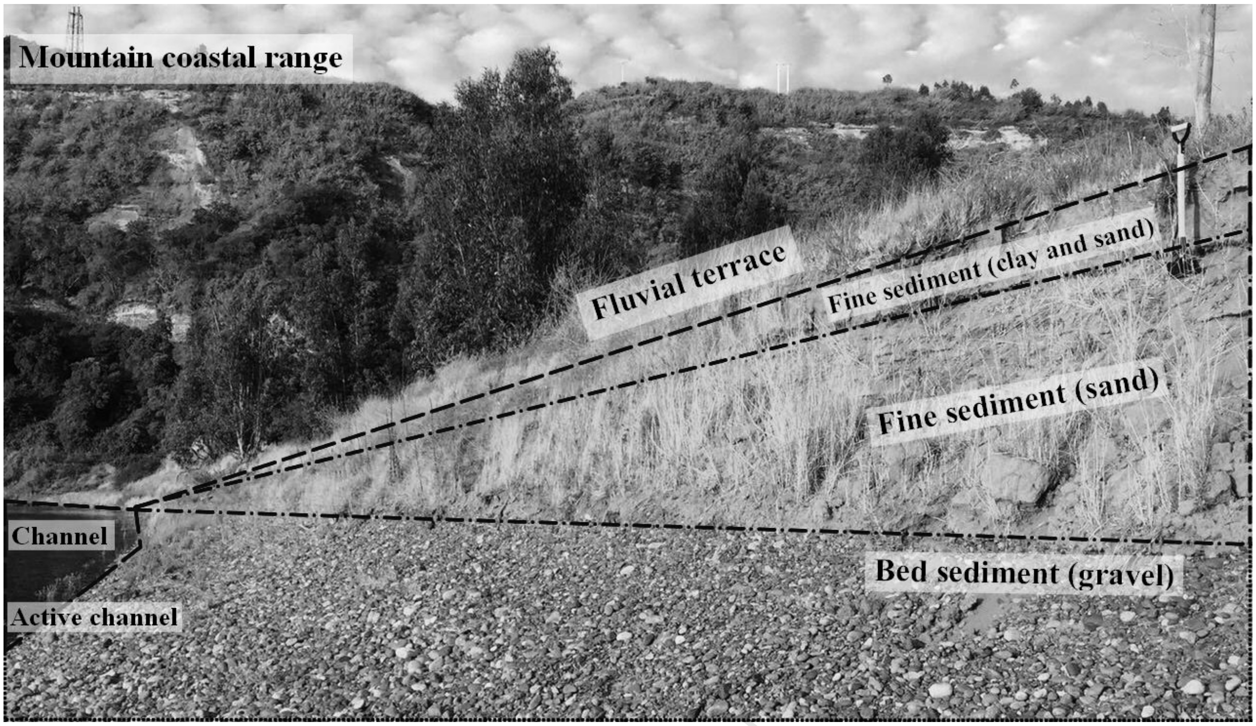
Mountain coastal range
Fluvial terrace
Fine sediment (clay and sand)
Fine sediment (sand)
Channel
Active channel
Bed sediment (gravel)

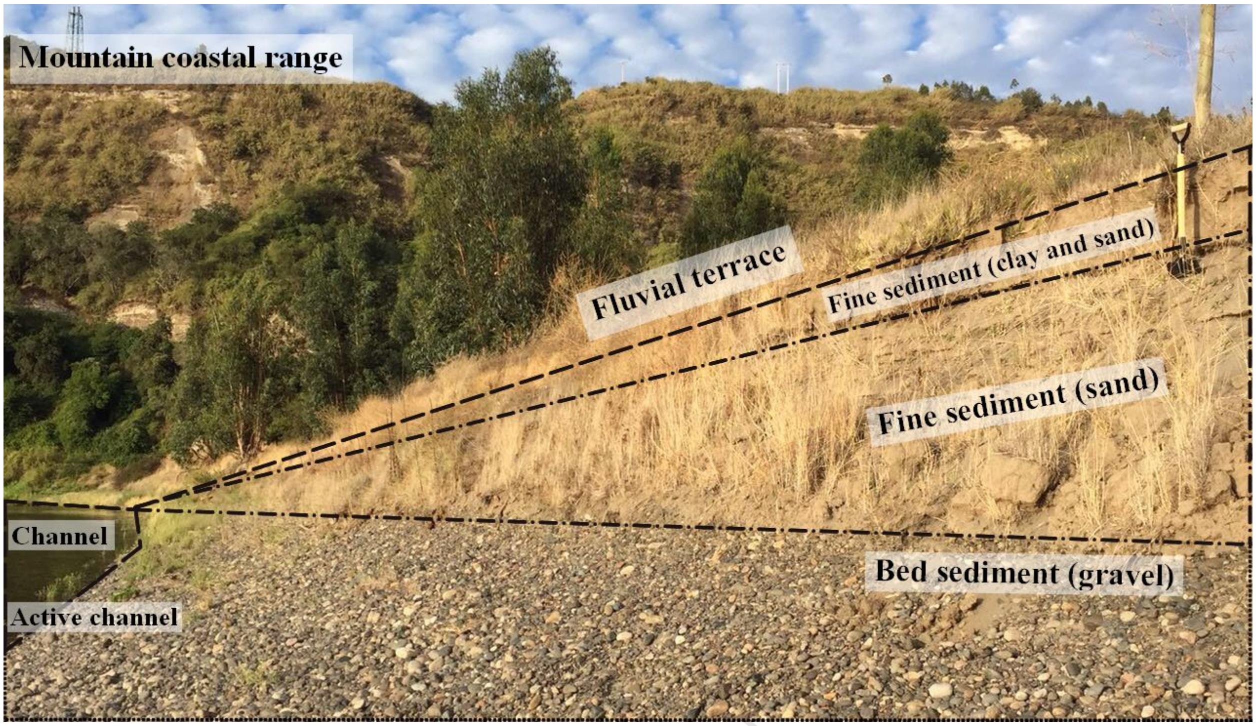
Mountain coastal range
Fluvial terrace
Fine sediment (clay and sand)
Fine sediment (sand)
Channel
Active channel
Bed sediment (gravel)

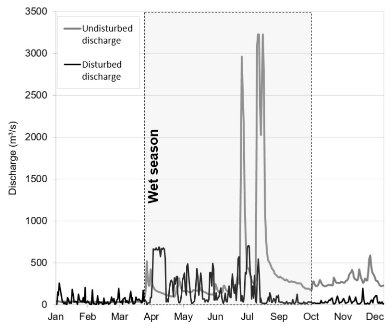

Undisturbed discharge
Disturbed discharge
Wet season
Discharge (m³/s)
3500
3000
2500
2000
1500
1000
500
0
Jan
Feb
Mar
Apr
May
Jun
Jul
Sep
Oct
Nov
Dec

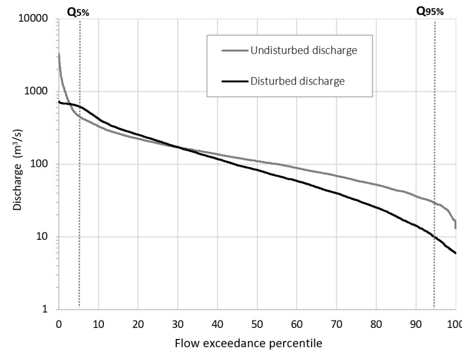

Q5%
Q95%
Undisturbed discharge
Disturbed discharge
Discharge (m³/s)
10000
1000
100
10
1
0
10
20
30
40
50
60
70
80
90
100
Flow exceedance percentile

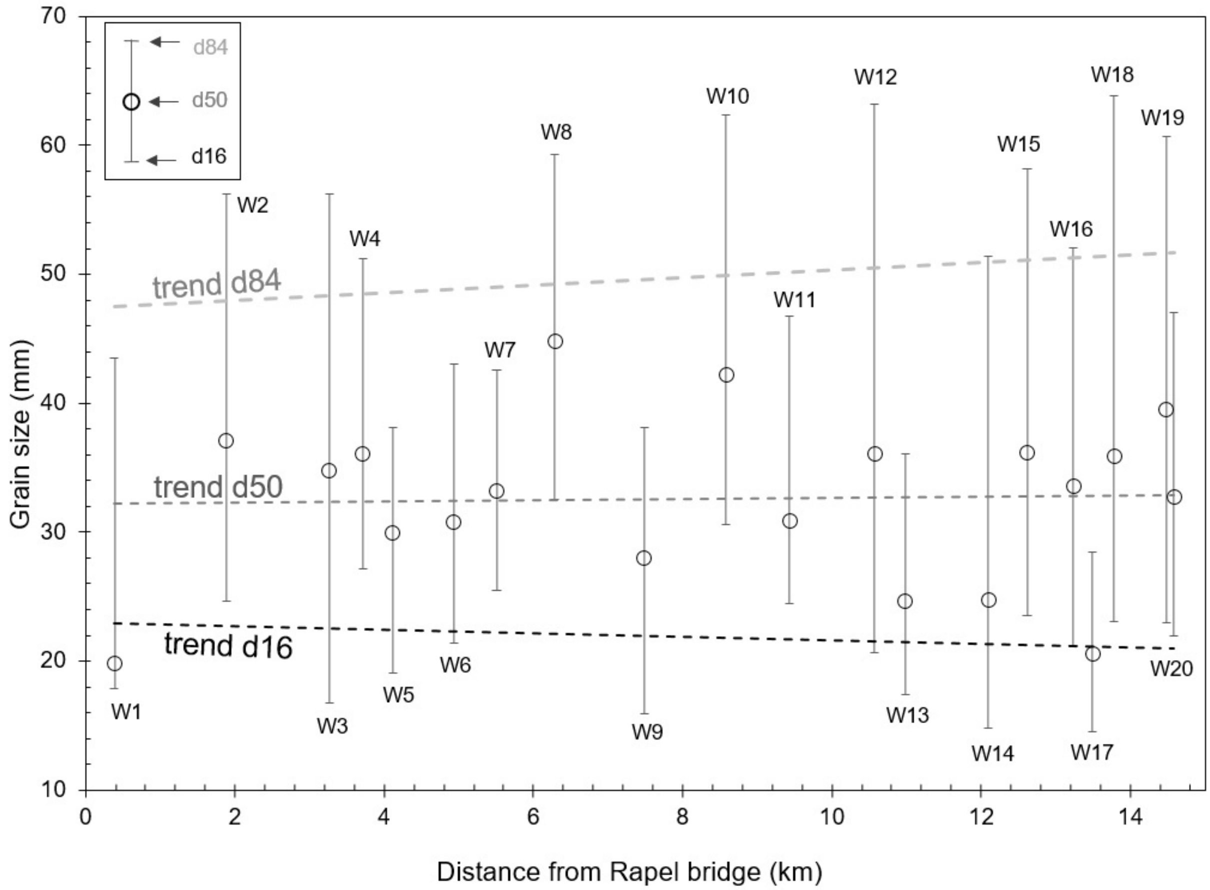

70
60
50
40
30
20
10
0
2
4
6
8
10
12
14
d84
d50
d16
trend d84
trend d50
trend d16
W1
W2
W3
W4
W5
W6
W7
W8
W9
W10
W11
W12
W13
W14
W15
W16
W17
W18
W19
W20
Grain size (mm)
Distance from Rapel bridge (km)

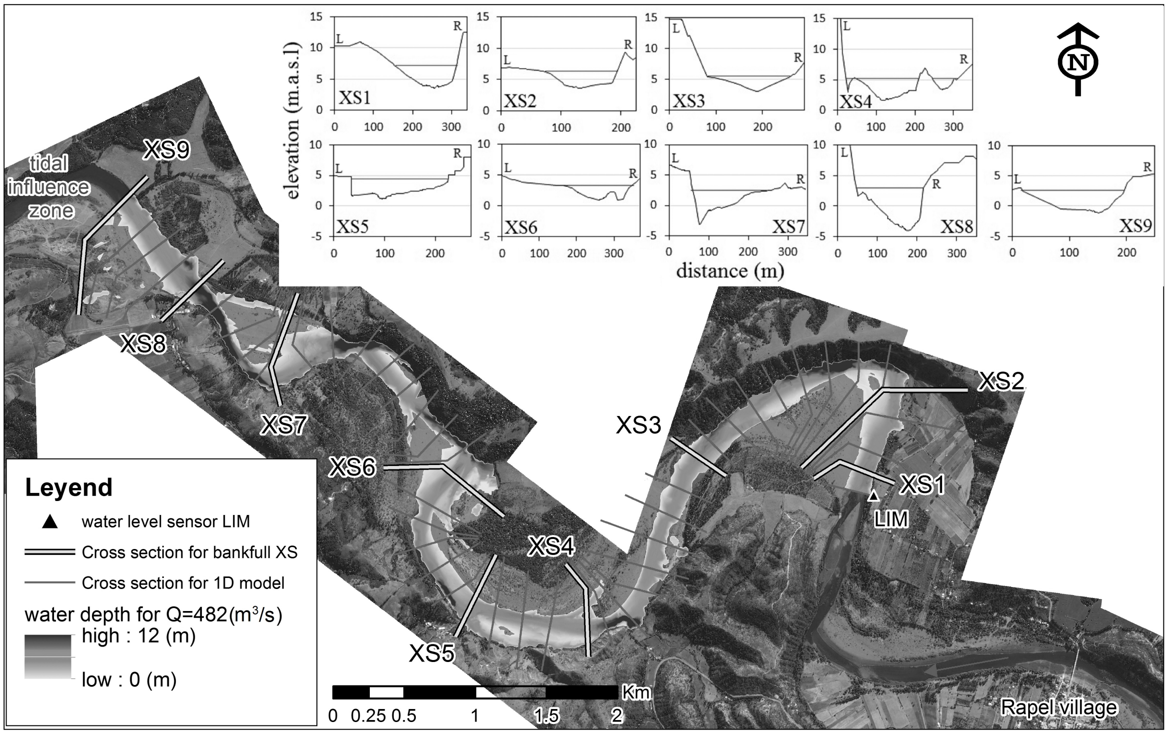

elevation (m.a.s.l)
distance (m)
XS1
XS2
XS3
XS4
XS5
XS6
XS7
XS8
XS9
L
R
N
tidal influence zone
LIM
Leyend
water level sensor LIM
Cross section for bankfull XS
Cross section for 1D model
water depth for Q=482(m³/s)
high : 12 (m)
low : 0 (m)
Km
0 0.25 0.5 1 1.5 2
Rapel village

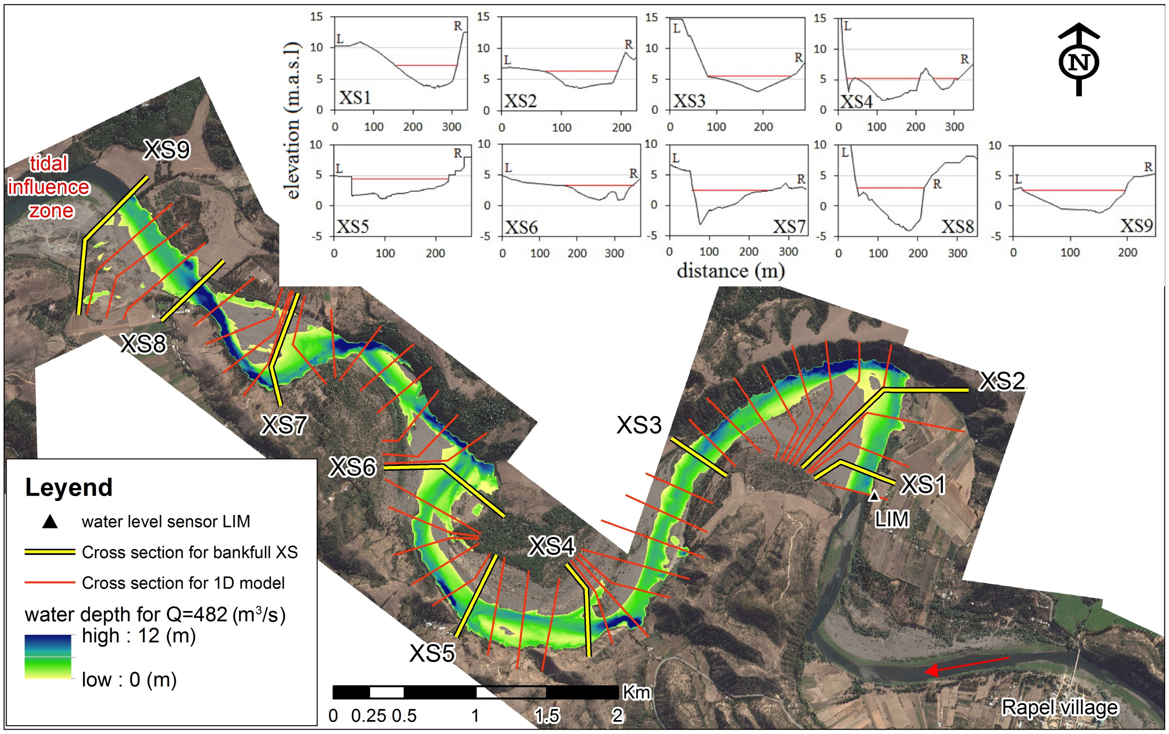

elevation (m.a.s.l)
distance (m)
XS1
XS2
XS3
XS4
XS5
XS6
XS7
XS8
XS9
L
R
tidal influence zone
LIM
Rapel village
Leyend
water level sensor LIM
Cross section for bankfull XS
Cross section for 1D model
water depth for Q=482 (m3/s)
high : 12 (m)
low : 0 (m)
0 0.25 0.5 1 1.5 2 Km
N

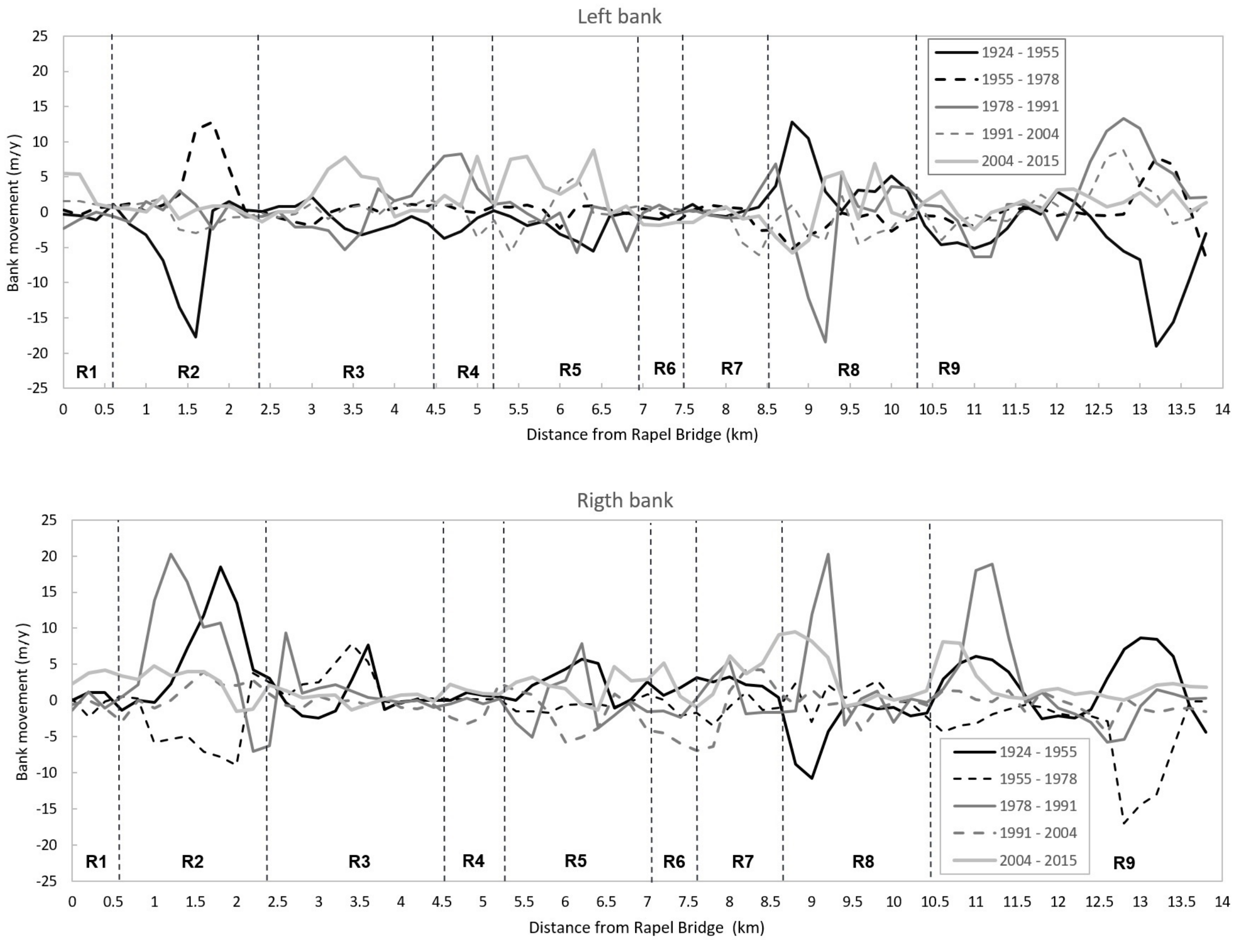
Left bank
Bank movement (m/y)
Distance from Rapel Bridge (km)
1924 - 1955
1955 - 1978
1978 - 1991
1991 - 2004
2004 - 2015
R1
R2
R3
R4
R5
R6
R7
R8
R9
Rigth bank
Bank movement (m/y)
Distance from Rapel Bridge (km)

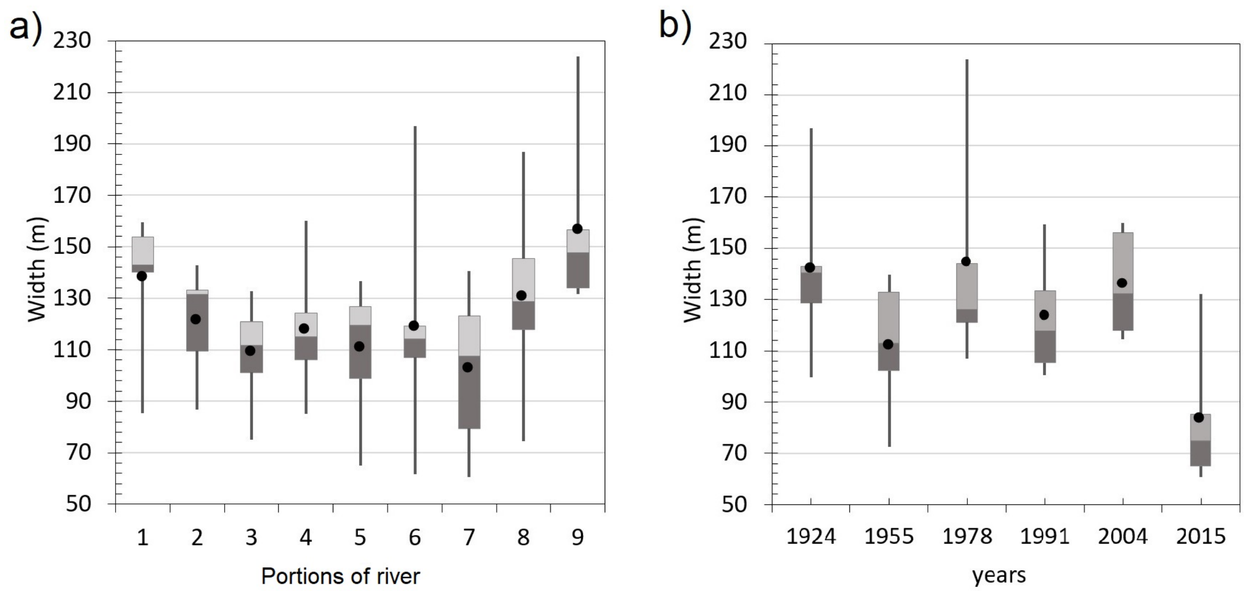
a)
230
210
190
170
150
130
110
90
70
50
Width (m)
1 2 3 4 5 6 7 8 9
Portions of river
b)
230
210
190
170
150
130
110
90
70
50
Width (m)
1924 1955 1978 1991 2004 2015
years

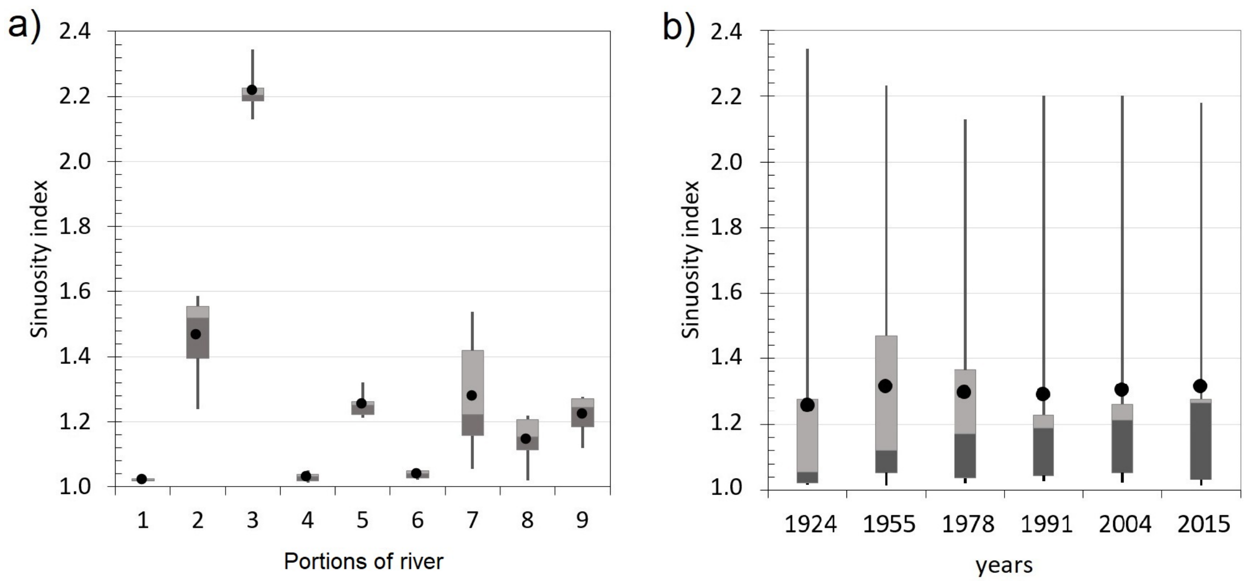
a)
2.4
2.2
2.0
1.8
1.6
1.4
1.2
1.0
Sinuosity index
1 2 3 4 5 6 7 8 9
Portions of river
b)
2.4
2.2
2.0
1.8
1.6
1.4
1.2
1.0
Sinuosity index
1924 1955 1978 1991 2004 2015
years

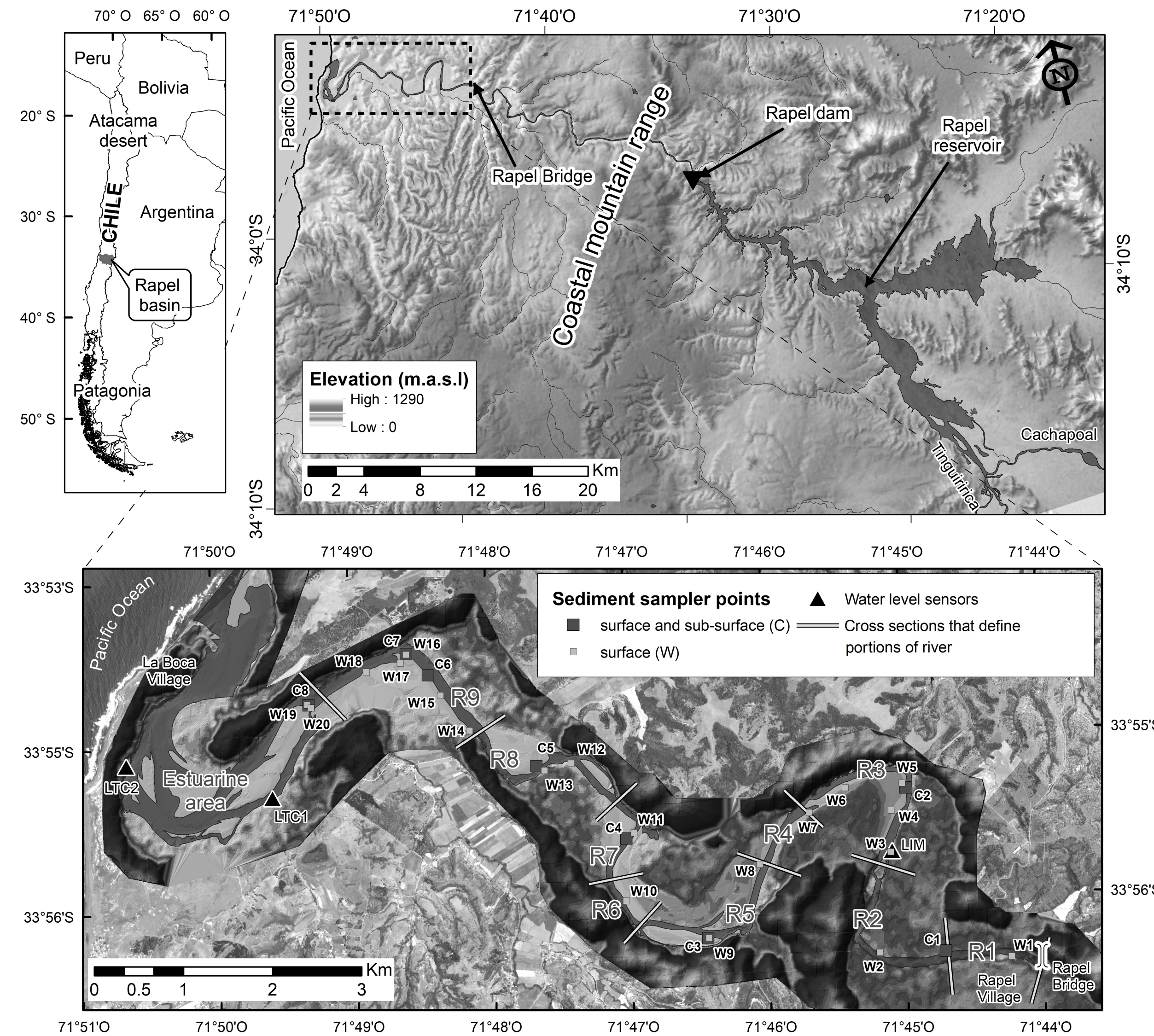

Peru
Bolivia
Atacama desert
CHILE
Argentina
Rapel basin
Patagonia
Pacific Ocean
Rapel Bridge
Coastal mountain range
Rapel dam
Rapel reservoir
Elevation (m.a.s.l)
High : 1290
Low : 0
Km
Cachapoal
Tinguiririca
La Boca Village
Estuarine area
LTC1
LTC2
Sediment sampler points
surface and sub-surface (C)
surface (W)
Water level sensors
Cross sections that define portions of river
Rapel Village
Rapel Bridge
LIM

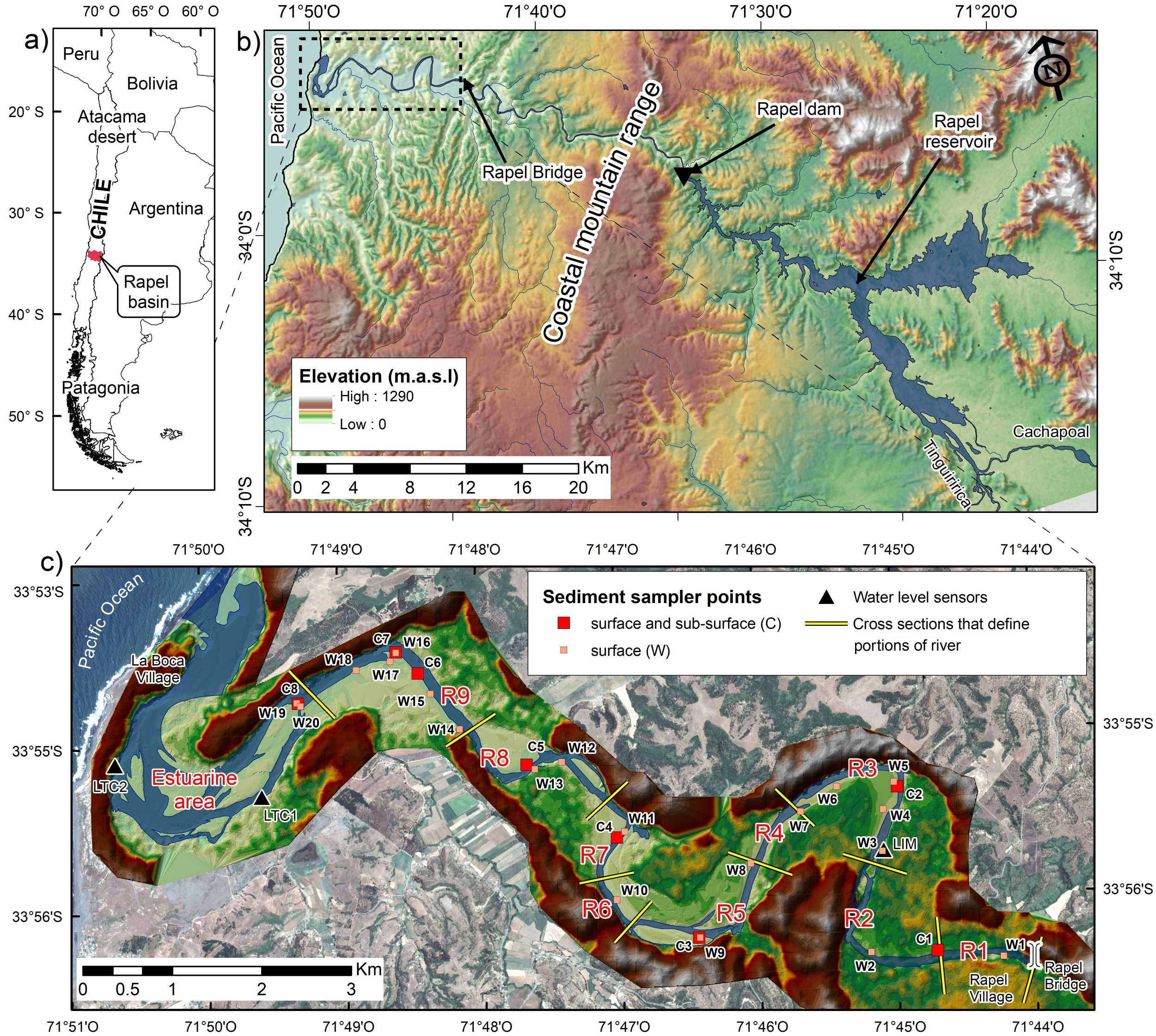
a)
Peru
Bolivia
Atacama desert
CHILE
Argentina
Rapel basin
Patagonia
b)
Pacific Ocean
Rapel Bridge
Coastal mountain range
Rapel dam
Rapel reservoir
Elevation (m.a.s.l)
High : 1290
Low : 0
Cachapoal
Tinguiririca
Km
c)
Pacific Ocean
La Boca Village
Estuarine area
LTC2
LTC1
Sediment sampler points
surface and sub-surface (C)
surface (W)
Water level sensors
Cross sections that define portions of river
LIM
Rapel Village
Rapel Bridge
Km

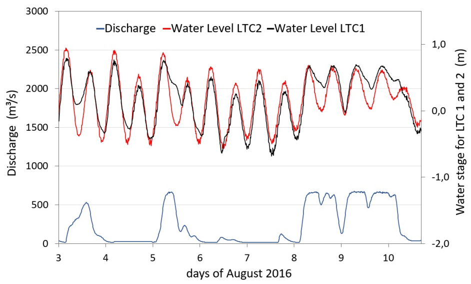
Discharge
Water Level LTC2
Water Level LTC1
Discharge (m³/s)
Water stage for LTC 1 and 2 (m)
days of August 2016
3000
2500
2000
1500
1000
500
0
1,0
0,0
-1,0
-2,0
3
4
5
6
7
8
9
10

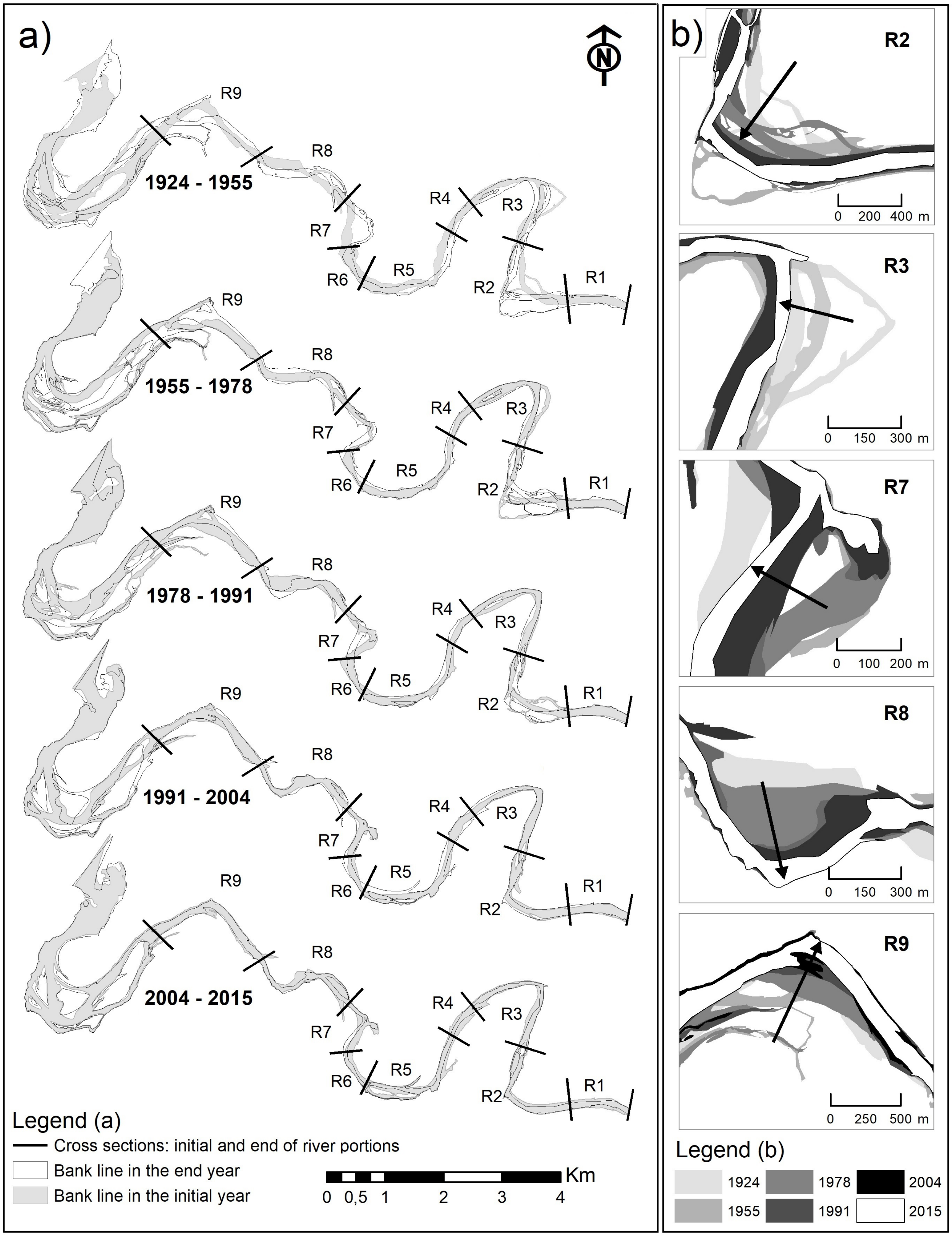
a)
N
R9
R8
1924 - 1955
R7
R6
R5
R4
R3
R2
R1
1955 - 1978
1978 - 1991
1991 - 2004
2004 - 2015
Legend (a)
Cross sections: initial and end of river portions
Bank line in the end year
Bank line in the initial year
0 0,5 1 2 3 4 Km
b)
R2
0 200 400 m
R3
0 150 300 m
R7
0 100 200 m
R8
0 150 300 m
R9
0 250 500 m
Legend (b)
1924
1978
2004
1955
1991
2015

Highlights

- Hydromorphological diagnostic to assess changes on the hydrological flow regime, bed-sediments, and fluvial morphology
- Identifies and characterizes the hydromorphological changes produced along the Rapel River downstream by the first large dam built in Chile
- Morphological changes smaller than expected and stabilization of the channel